

The hydrological regime of a forested tropical Andean catchment

Kathryn E. Clark¹, Mark A. Torres², A. Joshua West², Robert G. Hilton³, Mark New^{4,1},
Aline B. Horwath⁵, Joshua B. Fisher⁶, Joshua M. Rapp^{7,8}, Arturo Robles Caceres⁹, and
Yadvinder Malhi¹

¹ Environmental Change Institute, School of Geography and the Environment, University of
Oxford, Oxford, UK.

(*correspondence: kathryn.clark23@gmail.com; current address: Department of Earth and
Environmental Sciences, University of Pennsylvania, Philadelphia, PA, USA)

² Department of Earth Sciences, University of Southern California, Los Angeles, CA, USA.

³ Department of Geography, Durham, Durham University, UK.

⁴ African Climate and Development Initiative, University of Cape Town, Rondebosch, Cape
Town, South Africa.

⁵ Department of Plant Sciences, Cambridge, University of Cambridge, UK.

⁶ Jet Propulsion Laboratory, California Institute of Technology, Pasadena, CA, USA.

⁷ Department of Biology, Wake Forest University, Winston Salem, NC, USA.

⁸ Current address: Department of Evolution and Ecology, University of California, Davis,
CA, USA.

⁹ Facultad de Ciencias Biológicas, Universidad Nacional de San Antonio Abad del Cusco,
Cusco, Peru.

32 Abstract

33 The hydrology of tropical mountain catchments plays a central role in ecological
34 function, geochemical and biogeochemical cycles, erosion and sediment production, and
35 water supply in globally important environments. There have been few studies quantifying
36 the seasonal and annual water budgets in the montane tropics, particularly in cloud forests.
37 We investigated the water balance and hydrologic regime of the Kosñipata **catchment** (basin
38 area 164.4 km²) over the period 2010-2011. The **catchment** spans over 2500 m in elevation in
39 the eastern Peruvian Andes and is dominated by tropical montane cloud forest with some
40 high elevation *puna* grasslands. Catchment wide rainfall was **3112±414** mm yr⁻¹, calculated
41 by calibrating Tropical Rainfall Measuring Mission (TRMM) 3B43 rainfall with rainfall data
42 from 9 meteorological stations in the **catchment**. Cloud water input to streamflow was
43 **316±116** mm yr⁻¹ (**9.2%** of total inputs), calculated from an isotopic mixing model using
44 deuterium excess (Dxs) and δD of waters. Field stream flow was measured in 2010 by
45 recording height and calibrating to discharge. River runoff was estimated to be **2796±126** mm
46 yr⁻¹. Actual evapotranspiration (AET) was **688±138** mm yr⁻¹, determined using the Priestley
47 and Taylor – Jet Propulsion Laboratory (PT-JPL) model. The overall water budget was
48 balanced within **1.6 ± 13.7** %. Relationships between monthly rainfall and river runoff follow
49 an anti-clockwise hysteresis through the year, with a persistence of high runoff after the end
50 of the wet season. The size of the soil- and shallow ground-water reservoir is most likely
51 insufficient to explain sustained dry season flow. Thus, the observed hysteresis in rainfall-
52 runoff relationships is best explained by sustained groundwater flow in the dry season, which
53 is consistent with the water isotope results that suggest persistent wet season sources to
54 stream flow throughout the year. These results demonstrate the importance of transient
55 groundwater storage in stabilizing the annual hydrograph in this region of the Andes.

56

57

58 1. Introduction

59 The routing of water from the eastern flank of the Andes determines the quantity and
60 quality of this economically and ecologically valuable resource for the region (Célleri and
61 Feyen, 2009; Barnett et al., 2005; Postel and Thompson, 2005) and impacts the
62 biogeochemical cycles and ecology of the lowland Amazon (McClain and Naiman, 2008;
63 Allegre et al., 1996; Stallard and Edmond, 1983). The Amazon River has the highest
64 discharge of all of the world's rivers, at $6300 \text{ km}^3 \text{ yr}^{-1}$, with a very high runoff of 1000 mm
65 yr^{-1} over its watershed (Milliman and Farnsworth, 2011), and it contributes 20% of the global
66 water discharge to oceans (Beighley et al., 2009; Richey et al., 1990). The Andean portion of
67 the Amazon Basin ($> 500 \text{ m}$) represents an area of $623\,217 \text{ km}^2$ and covers $\sim 10\%$ of the
68 Amazon River Basin (McClain and Naiman, 2008). Although the water input from the Andes
69 to the Amazon is approximately proportional to areal coverage (10%) (McClain and Naiman,
70 2008; Dunne et al., 1998), the Andes are the dominant source of the Amazon's dissolved load
71 (McClain and Naiman, 2008; Gaillardet et al., 1999; Guyot et al., 1996), and contribute 80-
72 90% of its suspended sediment (Richey et al., 1986; Meade et al., 1985; Gibbs, 1967). Steep
73 high elevation Andean slopes are a particularly important source of material delivered to the
74 lowland Amazon (Lowman and Barros, 2014). Information about Andean river discharge,
75 flow sources, and flow routing is thus critical for understanding the suspended sediment
76 fluxes and chemical weathering processes of the Amazon River (Bouchez et al., 2012;
77 Wittmann et al., 2011; Guyot et al., 1996), for quantifying how the Andes contribute to
78 carbon and nutrient cycles (Clark et al., 2013; Townsend-Small et al., 2008), and for
79 assessing the aquatic ecology of the region (Anderson and Maldonado-Ocampo, 2011; Ortega
80 and Hidalgo, 2008). Hydrologic information is particularly important for understanding
81 related responses to changes in climate and land-use.

82 Despite this importance, the dynamics of Andean hydrology are still incompletely
83 characterized. This is especially true in Andean Tropical Montane Cloud Forest (TMCF),
84 which comprises a small area (Bubb et al., 2004) but is likely to contribute disproportionately
85 to the overall water balance of the region due to its topographic position that receives high
86 precipitation (Bruijnzeel et al., 2011; Killeen et al., 2007). The hydrology of TMCFs is of
87 particular interest because these forests are valuable and diverse ecosystems (Bruijnzeel et al.,
88 2010; Bubb et al., 2004; Myers et al., 2000) and have been shown to provide an important
89 supply of water to downstream regions, due in large part to their relatively high water yield,
90 i.e. high stream water output for a given precipitation input (Tognetti et al., 2010; Zadroga,
91 1981). TMCFs are unique hydrologic systems because of the additional water input from
92 cloud water interception (CWI) and because frequent fog occurrence may lower incoming
93 solar radiation, increasing humidity and potentially lowering evapotranspiration (ET)
94 (Giambelluca and Gerold, 2011; McJannet et al., 2010; Zadroga, 1981).

95 Transient groundwater storage may play a significant role in mountain hydrological
96 systems (Andermann et al., 2012; Calmels et al., 2011; Tipper et al., 2006). The importance
97 of groundwater in TMCF hydrology has recently been highlighted by studies in a Mexican
98 TMCF, where groundwater was shown to stabilize the rainfall-runoff response (Muñoz-
99 Villers and McDonnell, 2012), and in an Andean TMCF in Ecuador, where considering the

100 effect of groundwater reservoirs was important for accurately predicting streamflow (Crespo
101 et al., 2012). Improved understanding of the extent to which groundwater stabilizes Andean
102 TCMF hydrology is likely to be important for accurately assessing how environmental
103 change, such as land use change or shifting cloud base, might affect hydrological functioning
104 in the Andes and downstream in the Amazon (Rapp and Silman, 2014; Crespo et al., 2012;
105 Bruijnzeel et al., 2011; Mulligan, 2010; Ataroff and Rada, 2000).

106 In this paper we evaluate stream discharge of the Kosñipata River, in a well-studied
107 region in the eastern Andes of Peru (Rapp and Silman, 2014; Halladay et al., 2012a; van de
108 Weg et al., 2012; Salinas et al., 2011; Girardin et al., 2010; Malhi et al., 2010), over a one-
109 year period. We compare discharge data to rainfall, CWI, and evapotranspiration estimates in
110 order to assess the water balance and hydrologic variability throughout the study year. We
111 determine rainfall from meteorology station data and TRMM datasets, and we estimate actual
112 evapotranspiration using meteorological driver data and the Priestley-Taylor Jet Propulsion
113 Laboratory (PT-JPL) model (Fisher et al., 2008). We use the distinct water isotope
114 composition of cloud and rain water to constrain the role of cloud water input. Stable water
115 isotopes, i.e. δD (‰) and $\delta^{18}O$ (‰), can be used to distinguish water sources due to distinct
116 fractionation that occurs during evaporation and condensation (Scholl et al., 2011; Froehlich
117 et al., 2002; Gat, 1996; Rozanski et al., 1993; Craig, 1961). Stable water isotopes have been
118 used in studies of cloud forest hydrology to deduce the contribution of wet season
119 precipitation to dry season streamflow (Guswa et al., 2007), estimate local water recycling
120 (Scholl et al., 2007; Rhodes et al., 2006), determine temporal and spatial variation of rainfall
121 (Windhorst et al., 2013), trace water paths through soil layers in a catchment (Goller et al.,
122 2005), evaluate water sources in stormflow (Muñoz-Villers and McDonnell, 2012), quantify
123 water mean transit time (Timbe et al., 2014), and examine ecohydrological processes
124 including seasonal water-plant relations (Goldsmith et al., 2012), and interactions between
125 fog and vegetation (Dawson, 1998). In this study, we extend the application of stable water
126 isotopes to constrain the contributions of different precipitation sources to annual streamflow,
127 and in the process we add valuable new water isotope data to a growing number of TCMF
128 studies in the Andes (Windhorst et al., 2013).

129 There are few similar studies evaluating the water budget in TCMF (Caballero et al.,
130 2013; Schellekens, 2006; Zadroga, 1981), with particularly few providing comprehensive
131 estimates of precipitation inputs (Schellekens, 2006). Our comprehensive analysis of the
132 sources and sinks in the Kosñipata catchment allows us to focus attention on the following
133 questions: 1) How well can the annual water budget of the Kosñipata catchment be closed
134 and what are the uncertainties? 2) What is the importance of baseflow, i.e. the constant
135 supply of water throughout the year, not associated with short term fluctuations due to
136 storms? 3) Are there any significant seasonal lags between rainfall and stream runoff, and
137 what are the causes of these lags? 4) What is the relative importance of rainfall and cloud
138 water in sustaining streamflow throughout the year? and 5) What are the roles of soil and
139 groundwater storage in determining seasonal patterns of river flow?

140

141 2. Study Area

142 | The Kosñipata catchment (13°3'37" S, 71°32'40" W) study area ranges from 1360 to
143 | 4000 meters above sea level (masl) (Fig. 1a). We focus on the Kosñipata River measured at
144 | the San Pedro gauging station, which drains an area of 164.4 km². In the supplementary
145 | section we present results from the nested Wayqecha sub-catchment that encompasses the
146 | headwaters of the Kosñipata River, draining an area of 48.5 km² (Table 1). Downstream of
147 | the study region, the river flows into the Alto Madre de Dios River which feeds the Madre de
148 | Dios River (Fig. 1b), a major tributary of the Amazon River (Fig. 1c). The geology of the
149 | study area is dominated by meta-sedimentary mudstones covering ~80% of the catchment
150 | with a plutonic intrusion comprising ~20% of the catchment (Table 1) (Carlotto Caillaux et
151 | al., 1996). The geological characteristics and vegetation of the catchment are generally
152 | representative of the larger eastern Andean region of southern Peru and northern Bolivia
153 | (INGEMMET, 2013; Consbio, 2011; Carlotto Caillaux et al., 1996).

154 | The climate of the Eastern Andes is influenced by the South American Low Level Jet
155 | (SALLJ), which carries humid winds west over Amazonia and then south along the Andean
156 | flank (Marengo et al., 2004). The Kosñipata catchment sits in a band of persistent cloudiness
157 | that runs along the Eastern Andes (Halladay et al., 2012a) and has high rainfall relative to the
158 | Andean regions to the north and to the south because of its location on an east-west kink of
159 | the Andean range that situates it perpendicular to the SALLJ (Killeen et al., 2007). Within the
160 | catchment, rainfall decreases with increasing elevation, from 5300 mm yr⁻¹ at 1500 masl
161 | down to 1560 mm yr⁻¹ at 3025 masl, near the treeline (Girardin et al., 2014; Huaraca Huasco
162 | et al., 2014) where down-valley winds collide with most air from Amazonia (Halladay et al.,
163 | 2012a). Due to orographic effects, rainfall is highest from 1000 to 1500 masl (Rapp and
164 | Silman, 2012). Note that lower total annual rainfall amounts were reported previously for this
165 | catchment (Lambs et al., 2012), but the data used in this previous study were incomplete for
166 | the locations where we recorded highest rainfall. Orographic fog (cf. Scholl et al. (2011))
167 | plays an important role in the Kosñipata catchment. Cloud base varies in height throughout
168 | the year, with the cloud base at its lowest in the dry season (June to August) (Halladay,
169 | 2011). In July (mid-dry season) the cloud base is >60% of the time >1800 masl and 30% of
170 | the time between 1500-1800 masl (Rapp and Silman, 2014). Nearby, in the Central Peruvian
171 | Andes on leeward slopes, intercepted evaporation (rainfall interception losses by the canopy)
172 | was 210 mm yr⁻¹ in the UMCF and 660 mm yr⁻¹ in the LMCF (Gomez-Peralta et al., 2008);
173 | similar ranges are expected in the Kosñipata catchment. Annual mean temperatures in the
174 | Kosñipata catchment range from ~19 °C at low elevations to ~12 °C at high elevations
175 | (Girardin et al., 2014; Huaraca Huasco et al., 2014) with an adiabatic air temperature lapse
176 | rate of 4.94 °C km⁻¹ of altitude (Girardin et al., 2010). The wet season is generally defined to
177 | be December to March, the wet-dry transition season to be April, the dry season to be May to
178 | September, and the dry-wet transition season to be October and November (Table S1). These
179 | terms are used in a relative sense in the Andes, since precipitation is still significant in the dry
180 | season.

181 | Cloud water interception has not been measured previously in this part of the Andes,
182 | but in other similar TMCs, CWI ranges from 50 to 1200 mm yr⁻¹ (Bruijnzeel et al., 2011). In

183 many perhumid TMCs (Holwerda et al., 2010a; Holwerda et al., 2010b; McJannet et al.,
184 2010; Schmid et al., 2010; McJannet et al., 2007; Eugster et al., 2006), CWI typically makes
185 up a smaller proportion of the total input compared to seasonal and drier areas where CWI is
186 often a more important component in the annual water budget (García-Santos and Bruijnzeel,
187 2011; Marzol-Jaén et al., 2010; Guswa et al., 2007; Mulligan and Burke, 2005).

188 The Kosñipata catchment is dominated by forest (~93%) with the remainder of the
189 area covered by high elevation grasslands called *puna* (Squeo et al., 2006) (Table 1)
190 (Consbio, 2011). The timberline, the lowest elevation at which trees do not grow, occurs at
191 3000 to 3600 masl with puna grasslands and shrubland at higher elevations (Gibbon et al.,
192 2010). The soils in the *puna* grasslands are usually saturated for ~8 months of the year
193 (November to June; I. Oliveras personal communication, 2013) due to relatively high
194 precipitation and low temperatures (Wilcox et al., 1988). Small areas of bare bedrock are
195 exposed at the highest elevations. In the forested area of the Kosñipata catchment, vegetation
196 consists of upper montane cloud forest from approximately 2000 to 3450 masl, and lower
197 montane cloud forest and lower montane tropical rainforest from approximately 1200 to 2000
198 masl (Consbio, 2011). The Kosñipata catchment is partially contained in Manu National
199 Park, where logging is prohibited. The soils in the forested parts of the catchment are
200 predominantly inceptisols (Asner et al., 2014). Soil water content varies temporally by < 15%
201 throughout the year and soil moisture ranges spatially from 21 to 71 % throughout the
202 catchment (Girardin et al., 2014; Huaraca Huasco et al., 2014; Teh et al., 2014). At lower
203 altitudes there are only short periods at mid-day at the driest time of year which show some
204 signs of moisture stress (Rapp and Silman, 2012).

205

206 3. Materials and Methods

207 3.1. Catchment wide rainfall estimates

208 Meteorological stations are located throughout the Kosñipata valley along an
209 altitudinal gradient from 887 to 3460 masl (Fig. 1a & 2a), distributed in various landcover
210 types and on a range of slopes and aspects (Table S2). Only data from the Wayqecha
211 meteorological station (at 2900 masl) were recorded over the full length of this river study, so
212 rainfall was estimated using the long-term monthly record from $0.25^\circ \times 0.25^\circ$ merged
213 Tropical Rainfall Measuring Mission (TRMM) data (TRMM, 2013) together with the long-
214 term monthly rainfall data from nine meteorological stations (Girardin et al., 2014; Huaraca
215 Huasco et al., 2014; ACCA, 2012; Rapp and Silman, 2012; SENAMHI, 2012).

216 The 3B43 v7a TRMM is a third level product with outputs in mm d^{-1} , which have
217 been converted to mm month^{-1} with an output each month from 1998 to 2012. The Kosñipata
218 catchment is situated entirely within one 3B43 TRMM tile, which covers an area of $\sim 730 \text{ km}^2$
219 centred at $12^\circ 7' 48'' \text{S}$, $71^\circ 38' 6'' \text{W}$ (Fig. 1a). The raw TRMM 3B43 data underestimates
220 rainfall in the Andes (Scheel et al., 2011; Bookhagen and Strecker, 2008). Indeed, in the case
221 of the Kosñipata catchment, TRMM 3B43 rainfall is an underestimate compared to nearly all
222 of the data from meteorological station rainfall gauges in the catchment and is most

223 | comparable to the meteorological stations at high elevations with low rainfall (Fig. 2a).
224 | Because of the apparent systematic bias, we did not use the TRMM data directly but instead
225 | calibrated the TRMM data using meteorological data to make ~~robust~~ catchment wide rainfall
226 | estimates. This had the advantage of allowing us to use the long-term TRMM record that
227 | covers periods of time when data is not available from the meteorological stations, since the
228 | latter only have sporadic coverage, ranging from 13 to 79 months (Table S2). Details of the
229 | calibration procedure we used are provided in the supplementary section.

230 | In order to make robust catchment wide rainfall estimates, rainfall loss due to wind
231 | around the rainfall gauge was estimated using wind data from available meteorological
232 | stations along the Trocha Union (“Union Trail”) at 3450, 2750, and 1800 masl and at San
233 | Pedro at 1500 masl (Table S2). Cup anemometers were located in the tree canopy at the same
234 | height as the rain gauges. Correction of rainfall using wind speed followed Equations 1 and 2
235 | in Holwerda et al. (2006). The mean and standard error of wind speed and wind-induced
236 | rainfall loss (%) were determined seasonally and annually (Table S3), and seasonal averages
237 | for wind-loss rainfall (%) were used to correct catchment wide rainfall (corresponding to an
238 | annual correction of $2.50 \pm 0.56\%$). This approach may underestimate some wind-loss rainfall
239 | since the correction may have been larger at some meteorological stations (e.g., 4.2% at
240 | Wayqecha), but precise wind data were only available at a few sites so it was not possible to
241 | make site-specific corrections for all of the rainfall data from individual meteorological
242 | stations.

243 | 3.2. Discharge and runoff measures

244 | This study is based on measurements of Kosñipata River discharge made over a one-
245 | year period (Fig. 1a & 3), focusing on the Kosñipata River gauging station located at San
246 | Pedro (13°3'37"S, 71°32'40"W), at 1360 masl. Field measurements consisted of river height,
247 | flow velocity, and cross-sectional area, which together allowed us to estimate discharge and
248 | runoff over the study period. For full details of the measurements and corrections see the
249 | supplementary section; a brief summary is provided here. River stage height was measured
250 | from January 2010 to February 2011 using a river logger (Global Water WL16 Data Logger,
251 | range 0- 9 m), recording river level every ~15 min. The instantaneous discharge associated
252 | with each height measurement was calculated based on calibrated stage-discharge
253 | relationships. Total monthly discharge was determined by summing over each month, and the
254 | monthly totals were converted into an instantaneous discharge ($\text{m}^3 \text{s}^{-1}$) for each month.
255 | Monthly, seasonal and annual discharge and runoff were determined from these values. There
256 | was a gap in the logger data of 31 days in the dry season between mid-July and early-August
257 | (Fig. 3); these gaps were filled by linear interpolation. This interpolation misses storms, but
258 | these should have little influence on the annual discharge because of low flow throughout this
259 | period of time. Baseflow was determined from mean daily discharge ($\text{m}^3 \text{s}^{-1}$) using the
260 | method outlined in Gustard et al. (1992). Base flow index (BFI) was calculated as the ratio of
261 | the total volume of baseflow divided by the total volume of streamflow.

262

263 3.3. Actual evapotranspiration estimates

264 Actual evapotranspiration (AET) was estimated using the ecophysiologicaly
265 downscaled PT-JPL (Priestley and Taylor – Jet Propulsion Laboratory) AET method
266 developed by Fisher et al. (2008). This method has been evaluated extensively throughout the
267 tropics (Fisher et al., 2009). The model is based on ecophysiological theory using traits that
268 are measurable in the field or remotely. It takes a bio-meteorological approach incorporating
269 the radiation based model from Priestley and Taylor (1972) to determine rates of actual
270 evapotranspiration. The model requires only four variables: normalised difference vegetation
271 index (NDVI), net radiation (R_n), maximum air temperature (T_{max}), and minimum relative
272 humidity (RH_{min}). [The PT-JPL model predicts three components of the evapotranspiration
273 budget: canopy transpiration \(\$AET_c\$ \), rainfall evaporation interception \(\$AET_i\$ \), and soil
274 evaporation \(\$AET_s\$ \).](#) Details of the parameter values selected for actual evapotranspiration
275 estimates are provided in the supplementary section.

276 3.4. Water isotope measurements

277 River water, rainfall, and cloud water were collected from 2009 to 2011 from a range
278 of elevations throughout the [catchment](#). River water was collected from the river surface,
279 passed through a 0.2 μ m nylon filter, and stored unpreserved in containers that prevented
280 evaporative loss (see supplement). Rainfall samples were collected at the time of river water
281 collection near the river gauge, with additional samples collected along an altitudinal transect
282 in the [catchment](#) between 1500 to 3600 masl (Table [S4a](#)). Cloud vapour was collected along
283 the altitudinal transect below the canopy using a cryogenic pump (Table [S4b](#)).

284 Isotopic analysis was carried out on the samples to determine δD (delta deuterium,
285 $^2H/^1H$, ‰), $\delta^{18}O$ (delta 18-oxygen, $^{18}O/^{16}O$, ‰) and deuterium excess (defined as $Dxs = \delta D -$
286 $8 \times \delta^{18}O$, in ‰), all reported to relative to Standard Mean Oceanic Water (SMOW).
287 Deuterium excess (Dxs), representing the offset from the meteoric water line (see
288 supplement), provides information about the source conditions of water vapour (Dansgaard,
289 1964). It is controlled by kinetic effects during evaporation, where a larger Dxs value is an
290 indicator of enhanced moisture recycling and a lower value indicates an enhanced
291 evaporative loss (Cappa et al., 2003; Salati et al., 1979).

292 River water, rainfall, and water vapour samples were analysed with a Picarro L1102-i
293 cavity ring down spectrometer (CRDS). River water and rainfall from 2011 were injected 5
294 times and the final 3 samples averaged. Precision (1σ) was 0.2‰ for $\delta^{18}O$ and 1‰ for δD ,
295 though some samples showed larger uncertainties. VSMOW and VSLAP standards were
296 analysed at the same time and were used to assess accuracy and precision of the instrument
297 between runs. Rainfall from 2009 and water vapour were injected 9 times and the final 6
298 samples averaged. Precision (1σ) was <0.1‰ for $\delta^{18}O$ and 1‰ for δD . Calibration of results
299 to VSMOW was achieved by analysing internal standards before and after each set of 7 to 8
300 samples. Internal standards SPIT, BOTTY, and DELTA were used to calibrate against
301 VSMOW. Additional analyses using Isotope Radio Mass Spectrometry (IRMS) were used as
302 a check on the CRDS results (see supplement).

303 4. Results

304 4.1. Catchment wide rainfall

305 The estimated annual wind-loss corrected rainfall for the 12-month study period
306 (February 2010 to January 2011) was 3112 ± 414 mm, or 90.8 ± 16.5 % of total water inputs
307 (3428 ± 430 mm) (Table 2), where uncertainties are propagated errors reported at one
308 standard deviation (the same convention is used throughout the text). Based on the long-term
309 calibrated TRMM record, the 15-year (1998 to 2012) mean annual rainfall was 2881 ± 124
310 mm, indicating that our river discharge measurements were made in a year with slightly
311 higher than average rainfall (Fig. 4; Table S5). The total rainfall contribution over the study
312 period was divided into 100 m altitudinal bins to evaluate how rainfall was distributed over
313 the catchment. Although most of the catchment area is located at mid to high elevation ranges
314 (~2400-3400 masl), maximum rainfall occurs at ~2400 masl (Fig. 2c).

315 4.2. Discharge and Runoff

316 The Kosñipata River basin at San Pedro, with a mean elevation of 2805 masl and an
317 area of 164.4 km^2 , was estimated to have a mean discharge of $14.6 \pm 0.7 \text{ m}^3 \text{ s}^{-1}$ and runoff of
318 2796 ± 126 mm (81.6 ± 11.0 % of total precipitation) over the 1-year study period (Table 2).
319 This value falls within the runoff range of 2100 to 3070 mm yr⁻¹ for 2 microcatchments in the
320 Ecuadorian Andes, with very similar vegetation cover and elevation (Crespo et al., 2011). In
321 the Kosñipata catchment, 52% of the annual flow was during the wet season, which covers
322 only 33% of the year (Table 2).

323 Baseflow was 2173 ± 133 mm of the annual total runoff. The base flow index (BFI) is
324 the ratio between the total baseflow volume and total streamflow volume. The BFI value for
325 the Kosñipata (77%) is consistent with the 2 Ecuadorian catchments discussed above, where
326 80% of annual flow was attributed to baseflow (Crespo et al., 2011).

327 4.3. Evapotranspiration

328 Actual evapotranspiration (AET) was estimated from the PT-JPL model (Fisher et al.,
329 2008) at 688 ± 138 mm (20.1 ± 4.8 % of total precipitation). In previous work in lowland
330 tropical forests, AET was estimated to be 1000-1300 mm yr⁻¹ (Bruijnzeel et al., 2011; Fisher
331 et al., 2009), while TMCFs were characterised by ET values more similar to the Kosñipata
332 catchment, between 545 and 1200 mm yr⁻¹ (Bruijnzeel et al., 2011). AET in TMCFs is
333 reduced because fog immersion in TMCFs reduces solar radiation and lowers the vapour
334 pressure deficit, resulting in lower atmospheric evaporative demand (McJannet et al., 2010;
335 Letts and Mulligan, 2005; Bruijnzeel and Veneklaas, 1998), and because wet leaf surfaces
336 lower transpiration and photosynthesis (Letts and Mulligan, 2005).

337 The Interception evaporation component of the PT-JPL model was not tested against
338 data because no data were available. However, the model has been tested against many
339 lowland tropical forest flux sites, where the total ET measured does include intercepted
340 evaporation (Fisher et al., 2008). In the Kosñipata catchment the PT-JPL model predicts

341 intercepted evaporation to be $226 \pm 45 \text{ mm yr}^{-1}$ in the UMCF, $324 \pm 65 \text{ mm yr}^{-1}$ in the LMCF,
342 and $104 \pm 21 \text{ mm yr}^{-1}$ in the puna/transition. This compares favourably with direct
343 intercepted evaporation estimated in the Yanchaga-Chemillen forests in the central Peruvian
344 Andes, where intercepted evaporation in UMCF contributed 210 mm yr^{-1} or 7.7% of the bulk
345 precipitation, and in LMCF it contributed 660 mm yr^{-1} or 33% of the bulk precipitation input
346 (Gomez-Peralta et al., 2008). Our basin-wide estimate of AET_i was $225 \pm 45 \text{ mm yr}^{-1}$ or $6.6 \pm$
347 1.6% of the bulk precipitation ($3428 \pm 430 \text{ mm yr}^{-1}$).

348 Sap flow was measured in tree trunks in the Wayqecha forest plot (2900 masl) for one
349 month from mid-July to mid-August 2008. These sap flow values were used in the soil-plant
350 atmospheric (SPA) model to predict a canopy transpiration rate of 53 mm month^{-1} (van de
351 Weg et al., 2014). For the same time period, using the same meteorological data, the PT-JPL
352 model predicted a canopy transpiration (AET_c) of 49 mm. These similarities suggest that
353 even though the PT-JPL model has not been deployed in TMCF previously, it provides a
354 reasonable estimate of canopy transpiration and intercepted evapotranspiration. Thus, we
355 allocate a maximum error of $\sim 20\%$ on AET.

356 **4.4. Isotopic analyses and mixing calculations**

357 Rainwater δD and $\delta^{18}O$ values display considerable seasonal variation whereas
358 variation with elevation during a given season is less pronounced (Table S4a; Fig. 5).
359 Rainwater δD and $\delta^{18}O$ values are highest during the dry season. Seasonal variation in Dxs is
360 minimal (Fig. 5). The $\delta^{18}O$ and δD of Kosñipata cloud water vapours are not clearly distinct
361 from rainwaters. This result departs from the isotopic enrichment found in cloud waters in
362 non-orographic settings, but similarity between cloud and rainwater isotopes has also been
363 found in the few cases of orographic cloud formation that have been studied (Scholl et al.,
364 2011). Despite the overlap in $\delta^{18}O$ and δD , the cloud water vapour samples from the
365 Kosñipata **catchment** have higher and more variable Dxs values than all of the rainwater
366 samples (Fig. 5; Table S4b).

367 Streamwater δD , $\delta^{18}O$ and Dxs values ranged from -94.8 to -64.9 ‰ , -14.5 to -10.9
368 ‰ , and 19.1 to 22.6 ‰ respectively (Table S6). A slight seasonality is apparent in stream
369 water isotopic composition, with slightly higher δD values during the dry season and dry-to-
370 wet season transition (Fig. 6a). A significant seasonal variation in Dxs in streamwater is not
371 apparent (Fig. 6b). See the supplementary section for full details on the δD , $\delta^{18}O$, and Dxs
372 isotope results.

373 Qualitative comparison between the Kosñipata River water isotope data and the
374 rainwater and cloud water isotope data suggests that, throughout the year, wet season
375 precipitation is the dominant contributor to river discharge (Fig. 5). As discussed below, this
376 probably results from the storage of wet season precipitation in groundwater that is released
377 to the stream over time. It is possible that isotopic enrichment may take place via evaporation
378 as water makes its way from precipitation to streamflow, either associated with throughfall
379 (e.g. Brodersen et al. (2000)) or in soils (e.g. Dawson and Ehleringer (1998); Thorburn et al.
380 (1993)). Such isotopic enrichment could bias inferences about water sources using isotopic

381 signatures. However, we note that any evaporative enrichment would act to decrease the
382 relative contribution from wet season rainfall (the depleted source), supporting the qualitative
383 inference that wet season rainfall is the dominant source of streamflow throughout the year.
384 Moreover, the Kosñipata streamwaters appear to have little geochemical imprint of
385 evaporation. Chloride concentrations provide a conservative tracer that should be enriched
386 during evaporation; in the Kosñipata samples, Cl concentrations are similar in rainwater (2-
387 20 μM) and streamwater (2-12 μM) (Torres et al., in review). Kosñipata stream waters also
388 lie on the same local meteoric water line as rainwater (see Supplement), with no evidence for
389 relative D-depletion that may be expected during evaporation.

390 To quantitatively constrain the relative contributions of different water sources to
391 river discharge, a three end-member mixing model was used (see supplementary info for
392 details). In this model, mixing between wet season precipitation, dry season precipitation, and
393 dry season cloud water vapour is considered along with observed variability in the isotopic
394 compositions of each of these end-members (i.e. Phillips and Gregg (2001)). Since we
395 assume minimal evaporative enrichment of water isotopes during runoff generation, the
396 results of this model provide a minimum constraint on the contribution from wet season
397 rainfall. Results of the three end-member mixing calculations are distributions of possible
398 end-member contributions (Fig. 6c to f). For individual samples, mean contributions of wet
399 season rainfall, dry season rainfall, and cloud water vapour to river discharge range from 46-
400 67%, 19-33%, and 7-31% respectively (Fig. 6f; Table S7). Similarly, the maximum likely
401 contributions of each source to a single sample, which we define as the 95th percentile value
402 of the distributions from our mixing calculations, range from 66-87%, 38-60%, and 19-52%
403 for wet season precipitation, dry season precipitation, and cloud water vapour respectively
404 (Fig. 6c to f). It is worth noting that only two samples ($n = 62$) show mean and maximum
405 likely contributions of cloud water vapour greater than 18% and 40% respectively (Fig. 6f;
406 Table S7). These contributions calculated from the water isotope mixing model reflect the
407 ultimate source of the water to stream runoff, with storage and mixing in groundwater likely
408 to be an important intermediary but one which would not affect the source partitioning.

409 **4.5. Cloud water in streamflow**

410 Isotopic mixing calculations constrain the statistically most likely cloud water vapour
411 contribution to between 7 and 31% of streamflow, with only 2 samples >18% (Table S7). All
412 samples, except for the two with the highest analytical uncertainties, show this range of cloud
413 water vapour contribution regardless of collection season (Figs. 6f and 7c). Based on our
414 estimated monthly total river discharge and the average values for cloud water contribution in
415 each month, we estimate that total cloud water contribution to streamflow was $316 \pm 116 \text{ mm}$
416 yr^{-1} , using the 50th percentile values of the cloud water fraction and confidence intervals
417 defined by the 5th and 95th percentiles (Tables 3 & S7). Our estimated cloud water flux to the
418 river falls within the (admittedly very broad) range of CW interception fluxes measured in
419 TMCFs, which range from ~ 50 to 1200 mm yr^{-1} (Bruijnzeel et al., 2011; Bendix et al., 2008).
420 Compared to our annual discharge of $2796 \pm 126 \text{ mm}$, this means cloud water contributed
421 $11 \pm 4\%$ to annual streamflow.

422 | Our results suggest that cloud water appears to play a non-negligible contribution to
423 | stream runoff in the Kosñipata River, but that it remains secondary to precipitation inputs
424 | even during the dry season when rainfall is at its lowest and cloud immersion is most
425 | frequent. Cloud frequency is high in the catchment, with cloud cover > 70% year round
426 | (Halladay et al., 2012a). In the dry season the cloud base was > 1800 masl 40% of the time
427 | (Rapp and Silman, 2014). Cloud immersion is a key characteristic of tropical montane cloud
428 | forest (Bruijnzeel et al., 2011), and provides an important water source to the forest canopy
429 | and the diverse epiphyte community (Rapp and Silman, 2014; Bruijnzeel et al., 2011;
430 | Giambelluca and Gerold, 2011). However, it is possible that much of the intercepted water is
431 | transpired or evaporated directly from the canopy. Overall, cloud water contribution to stream
432 | runoff supplies a relatively constant proportion of total flow throughout the year and never
433 | dominates water inputs to the Kosñipata River, even during times of the lowest flow (Table
434 | 3).

435

436 | 5. Discussion

437 | 5.1. Water balance

438 | The annual water balance for the Kosñipata catchment can be described by the
439 | following equation (water inputs to the catchment on the left, losses from the catchment on
440 | the right):

$$441 | \text{Rainfall} + \text{CWI} = \text{AET} + \text{Runoff} + \text{Residual} \quad (1)$$

442 | Rainfall was estimated catchment-wide from TRMM and meteorological station rainfall at
443 | 3112 ± 414 mm yr⁻¹. Cloud water interception (CWI) was estimated from the isotope mixing
444 | model at 316 ± 116 mm yr⁻¹. Actual evapotranspiration (AET) was estimated from the PT-
445 | JPL model (Fisher et al., 2008) at 688 ± 138 mm yr⁻¹. Runoff was estimated from the gauging
446 | station at 2796 ± 126 mm yr⁻¹ (Fig. 8a). The residual of Eq (1) sums to -56 ± 469 mm, which is
447 | $-1.6 \pm 13.4\%$ of total annual water inputs through rainfall and CWI, indicating that any
448 | imbalance within our budget is within the estimated uncertainties of the water balance
449 | calculation.

450 | There are several additional structural uncertainties in our calculation of the water
451 | balance for the Kosñipata catchment. Rainfall was estimated for the catchment by calibrating
452 | TRMM rainfall using actual rainfall collected from 9 gauging stations. In the Kosñipata
453 | catchment there was a decrease of rainfall with an increase of elevation, corresponding to an
454 | average annual rainfall gradient of ~ -148 mm per hundred metres (Fig. 2a). It is possible that
455 | rainfall deviates from this trend along the altitudinal gradient because our results are limited
456 | to 9 meteorological stations dispersed over a large area (Fig. 1a). Intense localised storm
457 | activity also increases the chance of underestimating precipitation. The types of rain gauges
458 | used in the catchment (Table S2) are not ideal for cloud forests due to an underestimation of
459 | wind driven precipitation on steep slopes (Bruijnzeel et al., 2011; Frumau et al., 2011).
460 | Although we have corrected for wind losses (Holwerda et al., 2006), this correction method

461 | has not been tested specifically in the Kosñipata catchment. Stream runoff can be
462 | overestimated in mountain rivers due to an overestimation of velocity by taking
463 | measurements predominantly near the surface of the channel (Chen and Chiu, 2004; Thome
464 | and Zevenbergen, 1985). We have taken this under consideration and corrected surface
465 | velocity to estimate mean channel velocity (following Eq S1 in the Supplement), but it is
466 | possible that our runoff values remain overestimated. Taking these methodological
467 | uncertainties into consideration, our rainfall input value may be conservative, and stream
468 | runoff output value may be an upper bound.

469 | Improvements in our estimates of the water budget might be possible from additional
470 | work including: (1) characterising the interactions between topography, wind speed and the
471 | amounts of rainfall received on slopes with varying wind exposure; 2) measuring throughfall
472 | (crown drip) stable water isotope composition, which would make it possible to use isotope
473 | mass balance of different precipitation sources to test the calculated cloud water inputs, and
474 | 3) using distinct two component mass balance models to infer CWI for the different
475 | ecosystem types (puna/transition, UMCF and LMCF), i.e., as a variant of the wet canopy
476 | water budget approach of Holwerda et al. (2006) that was also used in Scholl et al. (2011).

477 | **5.2. Hysteresis**

478 | **5.2.1. Characterizing hysteresis**

479 | A monthly breakdown of the water balance shows the distribution of annual residual
480 | when water is going into storage (+) and when water is coming out of storage (- ; Fig. 9). The
481 | mid-wet season (January & February) was a time of recharge with positive residual values.
482 | This store was subsequently drained as discharge to stream runoff in the wet-dry transitional
483 | season (April) and most of the dry season (May to August), both of which showed negative
484 | residual values (Fig. 9). This seasonal shift (see Fig. 8) illustrates how rainfall stored during
485 | the wet season plays an important role in sustaining steady dry season runoff. The results of
486 | the isotope mixing analysis confirm this inference by showing that wet season rainfall is still
487 | prominent in contributing to streamflow in the dry season. Sources of streamflow from May
488 | to September 2010 were $61\pm 9\%$ from wet season rainfall, $25\pm 9\%$ from dry season rainfall,
489 | and $12\pm 7\%$ from cloud water (Table 3).

490 | At seasonal timescales, streamflow and baseflow in the Kosñipata catchment both
491 | follow an annual anti-clockwise hysteresis pattern (Fig. 10). This pattern is similar to that
492 | observed by Andermann et al. (2012) in the Nepalese Himalaya. In the wet season (December
493 | to March), the catchment wide rainfall in the Kosñipata catchment was greater than
494 | streamflow and baseflow (Fig. 10a & c). During the wet-dry transition season (April), and the
495 | start of the dry season (May and June) however, there was a switch and streamflow and
496 | baseflow were greater than rainfall. By the middle of the dry season (July and August)
497 | rainfall was equal to streamflow and baseflow. By the time of the late dry season
498 | (September), rainfall started to increase and was greater than streamflow and baseflow. The
499 | dry-wet transition season (October and November) had higher rainfall than streamflow and
500 | baseflow. Finally, in the early wet season (December to January) the cycle was completed

501 | where the contribution of rainfall dominated streamflow and baseflow (Fig. 10a & c). The
502 | annual anti-clockwise hysteresis was even more pronounced when streamflow and baseflow
503 | were compared to the rainfall gathered over the study period at the Wayqecha meteorological
504 | station at 2900 masl (Fig. 10b & d).

505 | The water isotope data support the indication of seasonal hysteresis observed in the
506 | water balance estimates. The relationship between river discharge and δD showed a seasonal
507 | clockwise hysteresis, but this was not observed in Dxs (Fig. 7a & b). Considering the
508 | observed end-member δD and Dxs compositions, this observation implies that there was
509 | seasonal variation in the relative contributions of wet and dry season rainfall but not cloud
510 | water vapour (Fig. 7c to e). The Monte-Carlo derived confidence intervals on the mixing
511 | results provide large ranges. However, the mean results (Fig. 7), which best represent each
512 | end-member composition, show a seasonal anti-clockwise hysteresis between river discharge
513 | and the mean contribution of wet-season precipitation that is consistent with the hysteresis
514 | observed in the water balance. Dry season and dry-wet transitional season runoff appear to be
515 | sustained by relatively lower, but still dominant, contributions from wet season precipitation
516 | (Fig. 7d). A corresponding variation in the contribution of dry season precipitation with
517 | discharge is also evident, whereby dry season and dry-wet transitional season runoff is
518 | composed of a larger proportion of dry season rainfall (Fig. 7e). The hysteresis in the mixing
519 | model results is attributable to the seasonal hysteresis in streamwater δD . No seasonal
520 | hysteresis in the contribution of cloud water interception to river discharge is apparent (Fig.
521 | 7c), consistent with no seasonal pattern in the streamwater Dxs.

522 | The consistent, annual anti-clockwise hystereses in both the water balance and the
523 | contribution from different sources inferred from the water isotopes indicate that there are
524 | important factors other than the storm runoff response that influenced hydrologic variability
525 | throughout the year in the Kosñipata catchment. The lag in runoff can be explained by a
526 | significant portion of wet season rainfall being stored, and then several months later
527 | discharged as runoff in the wet-dry transition and dry seasons (Fig. 10a & Table 2). The delay
528 | in rainfall to streamflow runoff helps provide water in the catchment at times of lower
529 | rainfall, stabilising dry season runoff.

530 | **5.2.2. Can soil water explain seasonal hysteresis?**

531 | There are several potential mechanisms causing a seasonal lag in streamflow. The
532 | water isotope data points to rainfall, rather than cloud water, as the primary source of water,
533 | but it is still unclear how rainfall is stored temporarily over the year. Shallow groundwater
534 | (i.e., lateral flow through soil layers) derived from accumulation of water in soils during the
535 | wet season may contribute to the delayed stream runoff. In the Kosñipata catchment, shallow
536 | groundwater may be sourced from drainage of saturated *puna* grassland soils. In *páramo*
537 | wetlands (a wetter mountain top biome) in the northern Andes of Ecuador, delayed
538 | groundwater has been shown to play an important role in dry season runoff (Buytaert and
539 | Beven, 2011). Tropical montane cloud forest soils, as found in a similar forest in Ecuador,
540 | can also be a potential source for delayed runoff over shorter periods of ~3.5 to ~9 weeks
541 | (Timbe et al., 2014).

542 | If seasonal variations in soil water content are sufficient to account for the seasonal
543 | lag in runoff in the Kosñipata, then:

$$A_{catchment} \times ED = A_{storage} \times d \times \Delta V \quad (2)$$

544 | where $A_{catchment}$ is the area of the drainage basin (m^2), ED is the seasonal excess discharge
545 | (mm) consisting of the sum of the monthly residual values from the wet-dry transitional
546 | season and most of the dry season (April to August; Fig. 9), $A_{storage}$ is the area of the basin
547 | covered in soil (m^2), d is depth of soil layer (m), and ΔV is the seasonal variation in soil water
548 | content that needs to occur to account for the excess discharge. Since the area of the
549 | catchment and area covered in soil are approximately the same, the area variables in Eq (2)
550 | cancel out. For our calculation, we assume mean soil depth (d) to be ~ 0.5 m, consistent with
551 | data from the Kosñipata catchment (Gibbon et al., 2010; Zimmermann et al., 2009). Typical
552 | soil water content in the TMCF and puna ranges spatially between 32 and 71 % (Teh et al.,
553 | 2014). Catchment wide seasonal variation (ΔV) of $< \sim 13\%$ was estimated using basin
554 | proportions (Fig. 2c) for each ecosystem type and soil moisture variations observed in each
555 | ecosystem. LMCF/LMRF dominates from 1350 to 2000 masl and comprises 8.3 % of the
556 | catchment -area, UMCF dominates from 2000 to 3450 masl and comprises 80.6% of the
557 | catchment, and transition/puna is found > 3450 masl, comprising 10.1 % of the catchment
558 | (Consbio, 2011). Temporal variability in soil moisture determined in past studies (Girardin et
559 | al., 2014; Huaraca Huasco et al., 2014; Teh et al., 2014) indicates $\Delta V = 5.4\%$ for
560 | LMCF/LMRF, $\Delta V = 15\%$ for UMCF and $\Delta V = 0.4\%$ for puna grasslands.

561 | Using an inferred catchment-wide $\Delta V = 12.6\%$, the total discharge contributed by soil
562 | water release, i.e. the right hand side of Eq (2), is estimated to be 65 mm. This suggests that
563 | water release from soil accounts for $\sim 17\%$ of the total seasonal ED in the Kosñipata river,
564 | with the remaining 310 mm (83%) not explained by seasonal storage and drainage of soils.
565 | How much more variable would soil water content have to be in order to explain all of the
566 | seasonal ED? By re-arranging Eq (2) as $\Delta V = ED/d$, we find that volumetric water content
567 | would need to vary by $\sim 75\%$ between seasons to fully account for our calculated seasonal
568 | excess discharge of 373 mm. This magnitude of required seasonal change is much greater
569 | than observed in any of the Kosñipata soils.

570 | 5.2.3. Importance of groundwater in hysteresis

571 | If soil water content changes are insufficient to account for the excess dry season
572 | discharge, the source of this excess discharge is likely to be groundwater stored within the
573 | fractured bedrock below the shallow soil layer. In central eastern Mexico, groundwater in the
574 | TMCF was found to be an important component of dry season runoff (Muñoz-Villers et al.,
575 | 2012). Groundwater occurs mostly in permeable bedrock and within fractures of
576 | impermeable bedrock (Jardine et al., 1999; Gascoyne and Kamineni, 1994; Todd and Mays,
577 | 1980). In the Nepal Himalayas, deep groundwater recharges through fractured bedrock
578 | containing aquifers several tens of meters deep and has a storage residence time of ~ 45 days
579 | (Andermann et al., 2012). Fracturing and the exposure of bedding planes through the process
580 | of uplift and erosion in the Kosñipata catchment (Carlotto Caillaux et al., 1996) could provide

581 conduits that aid in deep groundwater flow. In the Kosñipata, ~80% of the catchment area
582 consists of sedimentary mudstones and shale, and ~20% consists of plutonic intrusions (Table
583 1). Shale has a very low porosity and permeability (Domenico and Schwartz, 1998; Morris
584 and Johnson, 1967), but when fractured its porosity is greatly increased (Jardine et al., 1999).
585 Plutonic intrusions, as found in lower parts of the catchment, also have increased porosity as
586 a result of fracturing (Gascoyne and Kamineni, 1994). Thus we view deep fractured bedrock
587 as the likely transient storage reservoir that may explain the annual hydrograph in the
588 catchment. Further investigations into the hydrogeological characteristics of the soil profile
589 and weathered bedrock, such as saturated hydraulic conductivity (Kim et al., 2014; Kuntz et
590 al., 2011; Larsen, 2000) and specific yields of fractured rock types (Domenico and Schwartz,
591 1998) would help better elucidate the role of groundwater in sustained dry season baseflow.
592 Some of the seasonal storage of water could also be in valley fills, lower slope colluvial
593 deposits, peat and epiphyte biomass in the TMCF, and in saprolite, and better constraining
594 the potential water storage in such reservoirs would also be valuable further work.

595 The observation of a significant role for seasonal groundwater storage and release in
596 Kosñipata River has implications for understanding Andean water resources, predicting
597 flooding, and quantifying biogeochemical fluxes. The capacity for transient storage of water
598 in bedrock may be affected by land use changes, particularly if forests are removed and
599 resulting loss of forest soils reduces the “forest sponge” that facilitates water infiltration and
600 groundwater storage during the wet season (Bruijnzeel, 2004). Our observations are
601 important for assessing how the hydrologic system may respond to changing climate. The
602 rate of warming over the next 100 years in the region of the Kosñipata catchment is expected
603 to proceed an order of magnitude faster than the 1°C increase in temperature per 1000 years
604 during the Pleistocene-Holocene (Bush et al., 2004). The observation of upslope shift of plant
605 distributions already indicates a dramatic pace of change in the Kosñipata (Tovar et al., 2013;
606 Feeley et al., 2011; Hillyer and Silman, 2010). It remains unclear how patterns of rainfall and
607 cloud frequency have been changing and will change in the future (Halladay et al., 2012b;
608 Rapp and Silman, 2012), much less how the hydrologic system will respond, both to changes
609 in magnitude and in seasonality of precipitation sources. The baseline of water isotope data,
610 the partitioning of precipitation sources, and the conceptual framework presented in this
611 study offer the potential to help understand what hydrologic responses might be expected if
612 precipitation changes (e.g. as evaluated in Puerto Rico; (Scholl and Murphy, 2014)).
613 Moreover, further exploration and verification of the observations in this study, for example
614 by conducting long-term streamflow measurements (Larsen, 2000), considering longer-term
615 water budgets (Andermann et al., 2012), detailed analysis of stream hydrochemistry (Calmels
616 et al., 2011; Tipper et al., 2006), and/or analysing the isotopic composition of throughfall (i.e.
617 net precipitation), would strengthen understanding of how Andean TMCFs function
618 hydrologically today and how this function may evolve in the future.

619

620

621

622 6. Conclusions

623 An annual water budget for the Kosñipata catchment indicates that 3112 ± 414 mm
624 (90.8 ± 16.5% of total water inputs) was contributed to the catchment by rainfall, 316 ± 116 mm
625 (9.2 ± 3.6% of total water inputs) was supplied by cloud water, 2796 ± 126 mm (81.6 ± 11.0
626 % of total water inputs) was removed as streamflow, and 688 ± 138 mm (20.1 ± 4.8% of total
627 water inputs) was lost through actual evapotranspiration. The annual water budget balances at
628 -1.6 ± 13.4%. Annual stream runoff was composed of 60 ± 5% wet season rainfall, 26 ± 5%
629 dry season rainfall, and 11 ± 4% cloud water. Baseflow contributed 77% of the streamflow
630 over the one year of study. Runoff followed an annual anti-clockwise hysteresis with respect
631 to rainfall, exhibiting a lag in stream runoff that maintained stream water flow in the early dry
632 season. 61 ± 9% of dry season runoff originated as wet season rainfall. The contribution from
633 cloud water, although important to the TMCF ecology, plays a secondary role in river
634 streamflow (~10%) in this catchment, even during the low flow of the dry season. Seasonal
635 excess discharge measured throughout the wet-dry transitional season and dry season (April
636 to August) was ~373 mm, with storage and release of water in soil accounting for only ~17%
637 of this excess. Deep groundwater in fractured rock is probably the cause of the remaining
638 majority of the seasonal lag in stream runoff. The observation of seasonal groundwater
639 storage in this system has important implications for how land use and climate changes may
640 affect the hydrologic system in the Andes. Although significant over seasonal timescales,
641 there is no evidence for significant change in groundwater storage over the course of the one
642 year study period, given the balanced water budget and similar discharge and the beginning
643 and end of the study.

644

645

646 Author contribution

647 KEC, AJW, RGH, MN, and YM designed the study; KEC, ARC, ABH, and JMR carried out
648 the field work; KEC carried out data analysis; MAT analysed the water samples, developed
649 the mixing model and carried out the streamflow source simulations; and JBF developed the
650 PT-AET model. KEC and AJW prepared the manuscript with contributions from all the co-
651 authors.

652 Acknowledgements

653 This paper is a product of the Andes Biodiversity and Ecosystems Research Group
654 (ABERG). KEC was funded by the Natural Sciences and Engineering Research Council of
655 Canada (NSERC; 362718-2008 PGS-D3) and Clarendon Fund PhD scholarships. AJW is
656 supported to work in the Kosñipata by National Science Foundation (NSF) EAR 1227192.
657 YM is supported by the Jackson Foundation and by European Research Council Advanced
658 Investigator Grant 321121. We thank INRENA for providing permits to work in the study
659 area. We thank ACCA Peru (Wayqecha) and Incatererra (San Pedro) for field support; L.V.
660 Morales, R.J. Abarca Martínez, M.H. Yucra Hurtado, R. Paja Yurca, J. A. Gibaja Lopez, I.

661 Cuba Torres, J. Huamán Ovalle, A. Alfaro-Tapia, R. Butrón Loayza, J. Farfan Flores, D.
662 Ocampo, and D. Oviedo Licona for field assistance; [J. Selva-Espejo and W. Huaraca Huasco](#)
663 [for collection and provision of meteorological data, and SENHAMI for provision of national](#)
664 [weather station data](#). We thank L. Anderson for the TRMM 3B43 v7a data; [C. Girardin for](#)
665 [assistance with the water budget figure](#); S. Abele for [extraction of](#) the SENAMHI [rainfall](#)
666 data; M. Palace for the 2009 Quickbird image; G.P. Asner for use of the Carnegie Airborne
667 Observatory (CAO) DEM; [S. Waldron](#), S. Feakins and G. Goldsmith for constructive
668 comments and discussions; [L. A. Bruijnzeel and M. B. Gush for their thorough and](#)
669 [constructive reviews; G. Jewitt for editing the manuscript](#).

670

671

672

673 **References**

- 674 ACCA: Weather data San Pedro station, Asociación para la conservación de la cuenca Amazónica
675 <http://atrium.andesamazon.org/index.php>, (last access: April 2012), 2012.
- 676 Allegre, C. J., Dupre, B., Negrel, P., and Gaillardet, J.: Sr-Nd-Pb isotope systematics in Amazon and
677 Congo River systems: Constraints about erosion processes, *Chem. Geol.*, 131, 93-112,
678 [http://dx.doi.org/10.1016/0009-2541\(96\)00028-9](http://dx.doi.org/10.1016/0009-2541(96)00028-9), 1996.
- 679 Andermann, C., Longuevergne, L., Bonnet, S., Crave, A., Davy, P., and Gloaguen, R.: Impact of
680 transient groundwater storage on the discharge of Himalayan rivers, *Nat. Geosci.*, 5, 127-
681 132, <http://dx.doi.org/10.1038/NGEO1356>, 2012.
- 682 Anderson, E. P., and Maldonado-Ocampo, J. A.: A regional perspective on the diversity and
683 conservation of tropical Andean fishes, *Conserv. Biol.*, 25, 30-39,
684 <http://dx.doi.org/10.1111/j.1523-1739.2010.01568.x>, 2011.
- 685 Asner, G. P., Anderson, C. B., Martin, R. E., Knapp, D. E., Tupayachi, R., Sinca, F., and Malhi, Y.:
686 Landscape-scale changes in forest structure and functional traits along an Andes-to-Amazon
687 elevation gradient, *Biogeosciences*, 11, 843-856, <http://dx.doi.org/10.5194/bg-11-843-2014>,
688 2014.
- 689 Ataroff, M., and Rada, F.: Deforestation impact on water dynamics in a Venezuelan Andean cloud
690 forest, *Ambio.*, 29, 440-444, <http://dx.doi.org/10.1579/0044-7447-29.7.440>, 2000.
- 691 Barnett, T. P., Adam, J. C., and Lettenmaier, D. P.: Potential impacts of a warming climate on water
692 availability in snow-dominated regions, *Nature*, 438, 303-309,
693 <http://dx.doi.org/10.1038/nature04141>, 2005.
- 694 Beighley, R. E., Eggert, K. G., Dunne, T., He, Y., Gummadi, V., and Verdin, K. L.: Simulating hydrologic
695 and hydraulic processes throughout the Amazon River Basin, *Hydrol. Process.*, 23, 1221-
696 1235, <http://dx.doi.org/10.1002/hyp.7252>, 2009.
- 697 Bendix, J., Rollenbeck, R., Richter, M., Fabian, P., and Emck, P.: Climate Gradients in a Tropical
698 Mountain Ecosystem of Ecuador, in: *Gradients in a tropical mountain ecosystem of Ecuador*,
699 edited by: Beck, E., Bendix, J., Kottke, I., Makeschin, F., and Mosandl, R., *Ecological Studies*,
700 Springer Berlin Heidelberg, 63-73, 2008.
- 701 Bookhagen, B., and Strecker, M. R.: Orographic barriers, high-resolution TRMM rainfall, and relief
702 variations along the eastern Andes, *Geophys. Res. Lett.*, 35, L06403,
703 <http://dx.doi.org/10.1029/2007GL032011>, 2008.
- 704 Bouchez, J., Gaillardet, J., Lupker, M., Louvat, P., France-Lanord, C., Maurice, L., Armijos, E., and
705 Moquet, J.-S.: Floodplains of large rivers: Weathering reactors or simple silos?, *Chem. Geol.*,
706 332–333, 166-184, <http://dx.doi.org/10.1016/j.chemgeo.2012.09.032>, 2012.
- 707 Brodersen, C., Pohl, S., Lindenlaub, M., Leibundgut, C., and Wilpert, K. v.: Influence of vegetation
708 structure on isotope content of throughfall and soil water, *Hydrol. Process.*, 14, 1439-1448,
709 2000.
- 710 Bruijnzeel, L. A., and Veneklaas, E. J.: Climatic conditions and tropical montane forest productivity:
711 The fog has not lifted yet, *Ecology*, 79, 3-9, [http://dx.doi.org/10.1890/0012-9658\(1998\)079\[0003:CCATMF\]2.0.CO;2](http://dx.doi.org/10.1890/0012-9658(1998)079[0003:CCATMF]2.0.CO;2), 1998.
- 713 Bruijnzeel, L. A.: Hydrological functions of tropical forests: not seeing the soil for the trees?, *Agr
714 Ecosyst Environ*, 104, 185-228, <http://dx.doi.org/10.1016/j.agee.2004.01.015>, 2004.
- 715 Bruijnzeel, L. A., Kappelle, M., Mulligan, M., and Scatena, F. N.: Tropical montane cloud forests: state
716 of knowledge and sustainability perspectives in a changing world, in: *Tropical Montane
717 Cloud Forests. Science for Conservation and Management*, edited by: Hamilton, L. S.,
718 Bruijnzeel, L. A., and Scatena, F. N., Cambridge University Press, Cambridge, UK, 691-740,
719 2010.
- 720 Bruijnzeel, L. A., Mulligan, M., and Scatena, F. N.: Hydrometeorology of tropical montane cloud
721 forests: emerging patterns, *Hydrol. Process.*, 25, 465-498,
722 <http://dx.doi.org/10.1002/hyp.7974>, 2011.

723 Bubb, P., May, I., Miles, L., and Sayer, J.: Cloud forest agenda, UNEP-World Conservation Monitoring
724 Centre, UNEP World Conservation Monitoring Centre, Cambridge, UK, 2004.

725 Bush, M. B., Silman, M. R., and Urrego, D. H.: 48,000 Years of Climate and Forest Change in a
726 Biodiversity Hot Spot, *Science*, 303, 827-829, <http://dx.doi.org/10.1126/science.1090795>,
727 2004.

728 Buytaert, W., and Beven, K.: Models as multiple working hypotheses: Hydrological simulation of
729 tropical alpine wetlands, *Hydrol. Process.*, 25, 1784-1799,
730 <http://dx.doi.org/10.1002/hyp.7936>, 2011.

731 Caballero, L. A., Easton, Z. M., Richards, B. K., and Steenhuis, T. S.: Evaluating the bio-hydrological
732 impact of a cloud forest in Central America using a semi-distributed water balance model, *J*
733 *Hydrol Hydromech*, 61, 9-20b, <http://doi.doi.org/10.2478/jhh-2013-0003>, 2013.

734 Calmels, D., Galy, A., Hovius, N., Bickle, M., West, A. J., Chen, M. C., and Chapman, H.: Contribution
735 of deep groundwater to the weathering budget in a rapidly eroding mountain belt, Taiwan,
736 *Earth Planet. Sc. Lett.*, 303, 48-58, <http://dx.doi.org/10.1016/j.epsl.2010.12.032>, 2011.

737 Cappa, C. D., Hendricks, M. B., DePaolo, D. J., and Cohen, R. C.: Isotopic fractionation of water during
738 evaporation, *J. Geophys. Res.-Atmos.*, 108, 4525, <http://dx.doi.org/10.1029/2003JD003597>,
739 2003.

740 Carlotto Caillaux, V. S., Rodriguez, G., Fernando, W., Roque, C., Dionicio, J., and Chávez, R.: Geología
741 de los cuadrángulos de Urubamba y Calca, Instituto Geológica Nacional, Lima, Peru, 1996.

742 Célleri, R., and Feyen, J.: The hydrology of tropical Andean ecosystems: importance, knowledge
743 status, and perspectives, *Mt. Res. Dev.*, 29, 350-355, <http://dx.doi.org/10.1659/mrd.00007>,
744 2009.

745 Chen, Y.-C., and Chiu, C.-L.: A fast method of flood discharge estimation, *Hydrol. Process.*, 18, 1671-
746 1684, <http://dx.doi.org/10.1002/hyp.1476>, 2004.

747 Clark, K. E., Hilton, R. G., West, A. J., Malhi, Y., Gröcke, D. R., Bryant, C. L., Ascough, P. L., Robles
748 Caceres, A., and New, M.: New views on “old” carbon in the Amazon River: Insight from the
749 source of organic carbon eroded from the Peruvian Andes, *Geochem. Geophys. Geosy.*, 14,
750 1644-1659, <http://dx.doi.org/10.1002/ggge.20122>, 2013.

751 Consbio: Ecosistemas Terrestres de Peru (Data Basin Dataset) for ArcGIS, The Nature
752 Conservancy/NatureServe Covallis, Oregon, USA, (last access: April 2012), 2011.

753 Craig, H.: Standard for Reporting Concentrations of Deuterium and Oxygen-18 in Natural Waters,
754 *Science*, 133, 1833-1834, <http://dx.doi.org/10.1126/science.133.3467.1833>, 1961.

755 Crespo, P. J., Feyen, J., Buytaert, W., Bücker, A., Breuer, L., Frede, H. G., and Ramírez, M.: Identifying
756 controls of the rainfall–runoff response of small catchments in the tropical Andes (Ecuador),
757 *J. Hydrol.*, 407, 164-174, <http://dx.doi.org/10.1016/j.jhydrol.2011.07.021>, 2011.

758 Crespo, P. J., Feyen, J., Buytaert, W., Célleri, R., Frede, H.-G., Ramírez, M., and Breuer, L.:
759 Development of a conceptual model of the hydrologic response of tropical Andean micro-
760 catchments in Southern Ecuador, *Hydrol. Earth Syst. Sc.*, 9, 2475-2510,
761 <http://dx.doi.org/10.5194/hessd-9-2475-2012>, 2012.

762 Dansgaard, W.: Stable isotopes in precipitation, *Tellus*, 16, 436-468,
763 <http://dx.doi.org/10.1111/j.2153-3490.1964.tb00181.x>, 1964.

764 Dawson, T. E.: Fog in the California redwood forest: ecosystem inputs and use by plants, *Oecologia*,
765 117, 476-485, <http://dx.doi.org/10.1007/s004420050683>, 1998.

766 Dawson, T. E., and Ehleringer, J. R.: Plants, isotopes and water use: a catchment-scale perspective,
767 in: *Isotope tracers in catchment hydrology*, edited by: Kendall, C., and McDonnell, J. J.,
768 Elsevier, Amsterdam, 165-202, 1998.

769 Domenico, P. A., and Schwartz, F. W.: *Physical and chemical hydrogeology*, 2 ed., John Wiley & Sons,
770 New York, 1998.

771 Dunne, T., Mertes, L. A. K., Meade, R. H., Richey, J. E., and Forsberg, B. R.: Exchanges of sediment
772 between the flood plain and channel of the Amazon River in Brazil, *Geol. Soc. Am. Bull.*, 110,
773 450-467, [http://dx.doi.org/10.1130/0016-7606\(1998\)110<0450:eosbtf>2.3.co;2](http://dx.doi.org/10.1130/0016-7606(1998)110<0450:eosbtf>2.3.co;2), 1998.

774 Eugster, W., Burkard, R., Holwerda, F., Scatena, F. N., and Bruijnzeel, L. A.: Characteristics of fog and
775 fogwater fluxes in a Puerto Rican elfin cloud forest, *Agr. Forest Meteorol.*, 139, 288-306,
776 <http://dx.doi.org/10.1016/j.agrformet.2006.07.008>, 2006.

777 Farr, T. G., Rosen, P. A., Caro, E., Crippen, R., Duren, R., Hensley, S., Kobrick, M., Paller, M.,
778 Rodriguez, E., Roth, L., Seal, D., Shaffer, S., Shimada, J., Umland, J., Werner, M., Oskin, M.,
779 Burbank, D., and Alsdorf, D.: The Shuttle Radar Topography Mission, *Rev. Geophys.*, 45,
780 RG2004, <http://dx.doi.org/10.1029/2005RG000183>, 2007.

781 Feeley, K. J., Silman, M. R., Bush, M. B., Farfan, W., Cabrera, K. G., Malhi, Y., Meir, P., Revilla, N. S.,
782 Quisiyupanqui, M. N. R., and Saatchi, S.: Upslope migration of Andean trees, *J. Biogeogr.*, 38,
783 783-791, <http://dx.doi.org/10.1111/j.1365-2699.2010.02444.x>, 2011.

784 Fisher, J. B., Tu, K. P., and Baldocchi, D. D.: Global estimates of the land-atmosphere water flux
785 based on monthly AVHRR and ISLSCP-II data, validated at 16 FLUXNET sites, *Remote Sens.*
786 *Environ.*, 112, 901-919, <http://dx.doi.org/10.1016/j.rse.2007.06.025>, 2008.

787 Fisher, J. B., Malhi, Y., Bonal, D., Da Rocha, H. R., De Araujo, A. C., Gamo, M., Goulden, M. L., Hirano,
788 T., Huete, A. R., and Kondo, H.: The land-atmosphere water flux in the tropics, *Glob. Change*
789 *Biol.*, 15, 2694-2714, <http://dx.doi.org/10.1111/j.1365-2486.2008.01813.x>, 2009.

790 Froehlich, K., Gibson, J. J., and Aggarwal, P.: Deuterium excess in precipitation and its climatological
791 significance, *Proceeding of Study of Environmental Change Using Isotope Techniques*,
792 Vienna, Austria, 23-27 April 2001, IAEA-CSP-13/P, 54-66, 2002.

793 Frumau, K. F. A., Bruijnzeel, L. A., and Tobón, C.: Precipitation measurement and derivation of
794 precipitation inclination in a windy mountainous area in northern Costa Rica, *Hydrol.*
795 *Process.*, 25, 499-509, <http://dx.doi.org/10.1002/hyp.7860>, 2011.

796 Gaillardet, J., Dupré, B., Louvat, P., and Allègre, C. J.: Global silicate weathering and CO₂ consumption
797 rates deduced from the chemistry of large rivers, *Chem. Geol.*, 159, 3-30,
798 [http://dx.doi.org/10.1016/S0009-2541\(99\)00031-5](http://dx.doi.org/10.1016/S0009-2541(99)00031-5), 1999.

799 García-Santos, G., and Bruijnzeel, L. A.: Rainfall, fog and throughfall dynamics in a subtropical ridge
800 top cloud forest, National Park of Garajonay (La Gomera, Canary Islands, Spain), *Hydrol.*
801 *Process.*, 25, 411-417, <http://dx.doi.org/10.1002/hyp.7760>, 2011.

802 Gascoyne, M., and Kamineni, D.: The hydrogeochemistry of fractured plutonic rocks in the Canadian
803 Shield, *Applied Hydrogeology*, 2, 43-49, 1994.

804 Gat, J. R.: Oxygen and hydrogen isotopes in the hydrologic cycle, *Annu. Rev. Earth Pl. Sc.*, 24, 225-
805 262, 1996.

806 Giambelluca, T. W., and Gerold, G.: Hydrology and biogeochemistry of tropical montane cloud
807 forests, in: *Forest Hydrology and Biogeochemistry*, edited by: Levia, F. L., Carlyle-Moses, D.,
808 and Tanaka, T., Springer, Netherlands, 221-259, 2011.

809 Gibbon, A., Silman, M. R., Malhi, Y., Fisher, J. B., Meir, P., Zimmermann, M., Dargie, G. C., Farfan, W.
810 R., and Garcia, K. C.: Ecosystem carbon storage across the grassland-forest transition in the
811 high Andes of Manu National Park, Peru, *Ecosystems*, 13, 1097-1111,
812 <http://dx.doi.org/10.1007/s10021-010-9376-8>, 2010.

813 Gibbs, R. J.: Amazon River - Environmental factors that control its dissolved and suspended load,
814 *Science*, 156, 1734-1737, <http://dx.doi.org/10.1126/science.156.3783.1734>, 1967.

815 Girardin, C. A. J., Malhi, Y., Aragao, L. E. O. C., Mamani, M., Huasco, W. H., Durand, L., Feeley, K. J.,
816 Rapp, J., Silva-Espejo, J. E., Silman, M., Salinas, N., and Whittaker, R. J.: Net primary
817 productivity allocation and cycling of carbon along a tropical forest elevational transect in
818 the Peruvian Andes, *Glob. Change Biol.*, 16, 3176-3192, [http://dx.doi.org/10.1111/j.1365-](http://dx.doi.org/10.1111/j.1365-2486.2010.02235.x)
819 [2486.2010.02235.x](http://dx.doi.org/10.1111/j.1365-2486.2010.02235.x), 2010.

820 Girardin, C. A. J., Silva-Espejo, J. E., Doughty, C. E., Huaraca Huasco, W., Metcalfe, D. B., Durand-Baca,
821 L., Marthews, T. R., Aragao, L. E. O. C., Farfan Rios, W., García Cabrera, K., Halladay, K.,
822 Fisher, J. B., Galiano-Cabrera, D. F., Huaraca-Quispe, L. P., Alzamora-Taype, I., Equiluz-Mora,
823 L., Salinas-Revilla, N., Silman, M., Meir, P., and Malhi, Y.: Productivity and carbon allocation

824 in a tropical montane cloud forest of the Peruvian Andes, *Plant Ecology and Diversity*, 7, 107-
825 123, <http://dx.doi.org/10.1080/17550874.2013.820222>, 2014.

826 Goldsmith, G. R., Muñoz-Villers, L. E., Holwerda, F., McDonnell, J. J., Asbjornsen, H., and Dawson, T.
827 E.: Stable isotopes reveal linkages among ecohydrological processes in a seasonally dry
828 tropical montane cloud forest, *Ecohydrology*, 5, 779-790, <http://dx.doi.org/10.1002/eco.268>,
829 2012.

830 Goller, R., Wilcke, W., Leng, M. J., Tobschall, H. J., Wagner, K., Valarezo, C., and Zech, W.: Tracing
831 water paths through small catchments under a tropical montane rain forest in south Ecuador
832 by an oxygen isotope approach, *J. Hydrol.*, 308, 67-80,
833 <http://dx.doi.org/10.1016/j.jhydrol.2004.10.022>, 2005.

834 Gomez-Peralta, D., Oberbauer, S. F., McClain, M. E., and Philippi, T. E.: Rainfall and cloud-water
835 interception in tropical montane forests in the eastern Andes of Central Peru, *Forest Ecol
836 Manag*, 255, 1315-1325, <http://dx.doi.org/10.1016/j.foreco.2007.10.058>, 2008.

837 Gustard, A., Bullock, A., and Dixon, J.: Low flow estimation in the United Kingdom, *Low flow
838 estimation in the United Kingdom*, Institute of Hydrology, Wallingford, UKpp., 1992.

839 Guswa, A. J., Rhodes, A. L., and Newell, S. E.: Importance of orographic precipitation to the water
840 resources of Monteverde, Costa Rica, *Adv Water Resour*, 30, 2098-2112,
841 <http://dx.doi.org/10.1016/j.advwatres.2006.07.008>, 2007.

842 Guyot, J. L., Fillzola, N., Quintanilla, J., and Cortez, J.: Dissolved solids and suspended sediment yields
843 in the Rio Madeira basin, from the Bolivian Andes to the Amazon, *IAHS-AISH P.*, 236, 55-64,
844 1996.

845 Halladay, K.: Cloud characteristics of the Andes/Amazon transition zone, DPhil, School of Geography
846 and the Environment, University of Oxford, Oxford, UK, 260 pp., 2011.

847 Halladay, K., Malhi, Y., and New, M.: Cloud frequency climatology at the Andes/Amazon transition: 1.
848 Seasonal and diurnal cycles, *J. Geophys. Res.*, 117, D23102,
849 <http://dx.doi.org/10.1029/2012JD017770>, 2012a.

850 Halladay, K., Malhi, Y., and New, M.: Cloud frequency climatology at the Andes/Amazon transition: 2.
851 Trends and variability, *J. Geophys. Res.*, 117, D23103,
852 <http://dx.doi.org/10.1029/2012JD017789>, 2012b.

853 Hillyer, R., and Silman, M. R.: Changes in species interactions across a 2.5 km elevation gradient:
854 effects on plant migration in response to climate change, *Glob. Change Biol.*, 16, 3205-3214,
855 <http://dx.doi.org/10.1111/j.1365-2486.2010.02268.x>, 2010.

856 Holwerda, F., Burkard, R., Eugster, W., Scatena, F., Meesters, A., and Bruijnzeel, L.: Estimating fog
857 deposition at a Puerto Rican elfin cloud forest site: comparison of the water budget and
858 eddy covariance methods, *Hydrol Process*, 20, 2669-2692,
859 <http://dx.doi.org/10.1002/hyp.6065>, 2006.

860 Holwerda, F., Bruijnzeel, L. A., Muñoz-Villers, L. E., Equihua, M., and Asbjornsen, H.: Rainfall and
861 cloud water interception in mature and secondary lower montane cloud forests of central
862 Veracruz, Mexico, *J. Hydrol.*, 384, 84-96, <http://dx.doi.org/10.1016/j.jhydrol.2010.01.012>,
863 2010a.

864 Holwerda, F., Bruijnzeel, L. A., Oord, A. L., and Scatena, F. N.: Fog interception in a Puerto Rican elfin
865 cloud forest: a Wet-canopy Water budget approach, in: *Tropical Montane Cloud Forests:
866 Science for Conservation and Management*, edited by: Bruijnzeel, L. A., Scatena, F. N., and
867 Hamilton, L. S., Cambridge University Press, Cambridge, UK, 282-292, 2010b.

868 Huaraca Huasco, W., Girardin, C. A. J., Doughty, C. E., Metcalfe, D. B., Baca, L. D., Silva-Espejo, J. E.,
869 Cabrera, D. G., Aragão, L. E. O., Davila, A. R., Marthews, T. R., Huaraca-Quispe, L. P.,
870 Alzamora-Taype, I., Eguiluz-Mora, L., Farfan-Rios, W., Cabrera, K. G., Halladay, K., Salinas-
871 Revilla, N., Silman, M., Meir, P., and Malhi, Y.: Seasonal production, allocation and cycling of
872 carbon in two mid-elevation tropical montane forest plots in the Peruvian Andes, *Plant
873 Ecology and Diversity*, 1-2, 125-142, <http://dx.doi.org/10.1080/17550874.2013.819042>,
874 2014.

875 INGEMMET: GEOCATMIN - Geologia integrada por proyectos regionales, Instituto Geológico Minero
876 Metalúrgico Lima, Peru, (last access: March 2013), 2013.

877 Jardine, P. M., Sanford, W. E., Gwo, J. P., Reedy, O. C., Hicks, D. S., Riggs, J. S., and Bailey, W. B.:
878 Quantifying diffusive mass transfer in fractured shale bedrock, *Water Resour. Res.*, 35, 2015-
879 2030, 1999.

880 Killeen, T. J., Douglas, M., Consiglio, T., Jørgensen, P. M., and Mejia, J.: Dry spots and wet spots in the
881 Andean hotspot, *J. Biogeogr.*, 34, 1357-1373, [http://dx.doi.org/10.1111/j.1365-
882 2699.2006.01682.x](http://dx.doi.org/10.1111/j.1365-2699.2006.01682.x), 2007.

883 Kim, H., Bishop, J. K. B., Dietrich, W. E., and Fung, I. Y.: Process dominance shift in solute chemistry as
884 revealed by long-term high-frequency water chemistry observations of groundwater flowing
885 through weathered argillite underlying a steep forested hillslope, *Geochim Cosmochim Acta*,
886 140, 1-19, <http://dx.doi.org/10.1016/j.gca.2014.05.011>, 2014.

887 Kuntz, B. W., Rubin, S., Berkowitz, B., and Singha, K.: Quantifying solute transport at the Shale Hills
888 Critical Zone Observatory, *Vadose Zone J.*, 10, 843-857,
889 <http://dx.doi.org/10.2136/vzj2010.0130>, 2011.

890 Lambs, L., Horwath, A., Otto, T., Julien, F., and Antoine, P. O.: Isotopic values of the Amazon
891 headwaters in Peru: comparison of the wet upper Río Madre de Dios watershed with the dry
892 Urubamba-Apurimac river system, *Rapid Commun. Mass Sp.*, 26, 775-784,
893 <http://dx.doi.org/10.1002/rcm.6157>, 2012.

894 Larsen, M. C.: Analysis of 20th century rainfall and streamflow to characterize drought and water
895 resources in Puerto Rico, *Phys Geogr.*, 21, 494-521,
896 <http://dx.doi.org/10.1080/02723646.2000.10642723>, 2000.

897 Lehner, B., Verdin, K., and Jarvis, A.: New Global Hydrography Derived From Spaceborne Elevation
898 Data, *Eos Trans. AGU*, 89, 93-94, <http://dx.doi.org/10.1029/2008EO100001>, 2008.

899 Letts, M. G., and Mulligan, M.: The impact of light quality and leaf wetness on photosynthesis in
900 north-west Andean tropical montane cloud forest, *J. Trop. Ecol.*, 21, 549-557,
901 <http://dx.doi.org/10.1017/S0266467405002488>, 2005.

902 Lowman, L. E. L., and Barros, A. P.: Investigating Links between Climate and Orography in the central
903 Andes: Coupling Erosion and Precipitation using a Physical-statistical Model, *J Geophys Res-
904 Earth*, <http://dx.doi.org/10.1002/2013JF002940>, 2014.

905 Malhi, Y., Silman, M., Salinas, N., Bush, M., Meir, P., and Saatchi, S.: Introduction: Elevation gradients
906 in the tropics: laboratories for ecosystem ecology and global change research, *Glob. Change
907 Biol.*, 16, 3171-3175, <http://dx.doi.org/10.1111/j.1365-2486.2010.02323.x>, 2010.

908 Marengo, J. A., Soares, W. R., Saulo, C., and Nicolini, M.: Climatology of the low-level jet east of the
909 Andes as derived from the NCEP-NCAR reanalyses: Characteristics and temporal variability, *J.
910 Climate*, 17, 2261-2280, 2004.

911 Marzol-Jaén, M. V., Sanchez-Megía, J., and García-Santos, G.: Effects of fog on climatic conditions at
912 a sub-tropical montane cloud forest site in northern Tenerife (Canary Islands, Spain), in:
913 *Tropical Montane Cloud Forests: Science for Conservation and Management*, edited by:
914 Bruijnzeel, L. A., Scatena, F. N., and Hamilton, L. S., Cambridge University Press, Cambridge,
915 UK, 359-364, 2010.

916 McClain, M. E., and Naiman, R. J.: Andean influences on the biogeochemistry and ecology of the
917 Amazon River, *Bioscience*, 58, 325-338, <http://dx.doi.org/10.1641/b580408>, 2008.

918 McJannet, D., Wallace, J., and Reddell, P.: Precipitation interception in Australian tropical rainforests:
919 II. Altitudinal gradients of cloud interception, stemflow, throughfall and interception, *Hydrol.
920 Process.*, 21, 1703-1718, <http://dx.doi.org/10.1002/hyp.6346>, 2007.

921 McJannet, D. L., Wallace, J. S., and Reddell, P.: Comparative water budgets of a lower and an upper
922 montane cloud forest in the Wet Tropics of northern Australia, in: *Tropical Montane Cloud
923 Forests. Science for Conservation and Management*, edited by: Bruijnzeel, L. A., and Scatena,
924 F. N., Cambridge University Press, Cambridge, UK, 479-490, 2010.

925 Meade, R. H., Dunne, T., Richey, J. E., Santos, U. D., and Salati, E.: Storage and remobilisation of
926 suspended sediment in the lower Amazon River of Brazil, *Science*, 228, 488-490,
927 <http://dx.doi.org/10.1126/science.228.4698.488>, 1985.

928 Milliman, J. D., and Farnsworth, K. L.: Runoff, erosion, and delivery to the coastal ocean, in: *River
929 discharge to the coastal ocean: a global synthesis*, Cambridge University Press, Cambridge,
930 UK, 13-69, 2011.

931 Morris, D. A., and Johnson, A. I.: Summary of Hydrologic and Physical Properties of Rock and Soil
932 Materials, as Analyzed by the Hydrologic Laboratory of the US Geological Survey 1948-60,
933 Summary of Hydrologic and Physical Properties of Rock and Soil Materials, as Analyzed by
934 the Hydrologic Laboratory of the US Geological Survey 1948-60, US Government Printing
935 Office, Washington, USA, 46 pp., 1967.

936 Mulligan, M., and Burke, S. M.: FIESTA: Fog Interception for the Enhancement of Streamflow in
937 Tropical Areas, FIESTA: Fog Interception for the Enhancement of Streamflow in Tropical
938 Areas, for KCL/AMBIOTEK Contribution to DFID-FRP project R7991pp., 2005.

939 Mulligan, M.: Modelling the tropics-wide extent and distribution of cloud forest and cloud forest
940 loss, with implications for conservation priority, in: *Tropical Montane Cloud Forests. Science
941 for Conservation and Management*, edited by: Bruijnzeel, L. A., Scatena, F. N., and Hamilton,
942 L. S., Cambridge University Press, Cambridge, UK, 14-38, 2010.

943 Muñoz-Villers, L. E., Holwerda, F., Gómez-Cárdenas, M., Equihua, M., Asbjornsen, H., Bruijnzeel, L.
944 A., Marín-Castro, B. E., and Tobón, C.: Water balances of old-growth and regenerating
945 montane cloud forests in central Veracruz, Mexico, *J. Hydrol.*, 462, 53-66,
946 <http://dx.doi.org/10.1016/j.jhydrol.2011.01.062>, 2012.

947 Muñoz-Villers, L. E., and McDonnell, J. J.: Runoff generation in a steep, tropical montane cloud forest
948 catchment on permeable volcanic substrate, *Water Resour. Res.*, 48, W09528,
949 <http://dx.doi.org/10.1029/2011WR011316>, 2012.

950 Myers, N., Mittermeier, R. A., Mittermeier, C. G., Da Fonseca, G. A. B., and Kent, J.: Biodiversity
951 hotspots for conservation priorities, *Nature*, 403, 853-858,
952 <http://dx.doi.org/10.1038/35002501>, 2000.

953 Ortega, H., and Hidalgo, M.: Freshwater fishes and aquatic habitats in Peru: Current knowledge and
954 conservation, *Aquat. Ecosyst. Health*, 11, 257-271,
955 <http://dx.doi.org/10.1080/14634980802319135>, 2008.

956 Phillips, D. L., and Gregg, J. W.: Uncertainty in source partitioning using stable isotopes, *Oecologia*,
957 127, 171-179, <http://dx.doi.org/10.1007/s004420000578>, 2001.

958 Postel, S. L., and Thompson, B. H.: Watershed protection: Capturing the benefits of nature's water
959 supply services, *Natural Resources Forum*, 29, 98-108, [http://dx.doi.org/10.1111/j.1477-
960 8947.2005.00119.x](http://dx.doi.org/10.1111/j.1477-8947.2005.00119.x), 2005.

961 Priestley, C. H. B., and Taylor, R. J.: On the Assessment of Surface Heat Flux and Evaporation Using
962 Large-Scale Parameters, *Mon. Weather Rev.*, 100, 81-92, [http://dx.doi.org/10.1175/1520-
963 0493\(1972\)100<0081:otaosh>2.3.co;2](http://dx.doi.org/10.1175/1520-0493(1972)100<0081:otaosh>2.3.co;2), 1972.

964 Rapp, J. M., and Silman, M. R.: Diurnal, seasonal, and altitudinal trends in microclimate across a
965 tropical montane cloud forest, *Clim. Res.*, 55, 17-32, <http://dx.doi.org/10.3354/cr01127>,
966 2012.

967 Rapp, J. M., and Silman, M. R.: Epiphyte response to drought and experimental warming in an
968 Andean cloud forest [v2; ref status: indexed, <http://f1000r.es/3le>], *F1000Res.*, 3,
969 <http://dx.doi.org/10.12688/f1000research.3-7.v2>, 2014.

970 Rhodes, A. L., Guswa, A. J., and Newell, S. E.: Seasonal variation in the stable isotopic composition of
971 precipitation in the tropical montane forests of Monteverde, Costa Rica, *Water Resour. Res.*,
972 42, W11402, <http://dx.doi.org/10.1029/2005WR004535>, 2006.

973 Richey, J. E., Meade, R. H., Salati, E., Devol, A. H., Nordin, C. F., and Dossantos, U.: Water discharge
974 and suspended sediment concentrations in the Amazon River 1982-1984, *Water Resour.
975 Res.*, 22, 756-764, <http://dx.doi.org/10.1029/WR022i005p00756>, 1986.

- 976 Richey, J. E., Valarezo, C., Valarezo, C., and Valarezo, C.: Biogeochemistry of carbon in the Amazon
977 River, *Limnol. Oceanogr.*, 35, 352-371, 1990.
- 978 Rozanski, K., Araguás-Araguás, L., and Gonfiantini, R.: Isotopic Patterns in Modern Global
979 Precipitation, in: *Climate Change in Continental Isotopic Records*, edited by: Swart, P. K.,
980 Lohman, K. C., McKenzie, J., and Savin, S., American Geophysical Union, Washington, DC, 1-
981 36, 1993.
- 982 Salati, E., Dall'Olio, A., Matsui, E., and Gat, J. R.: Recycling of water in the Amazon basin: an isotopic
983 study, *Water Resour. Res.*, 15, 1250-1258, <http://dx.doi.org/10.1029/WR015i005p01250>,
984 1979.
- 985 Salinas, N., Malhi, Y., Meir, P., Silman, M., Roman Cuesta, R., Huaman, J., Salinas, D., Huaman, V.,
986 Gibaja, A., Mamani, M., and Farfan, F.: The sensitivity of tropical leaf litter decomposition to
987 temperature: results from a large-scale leaf translocation experiment along an elevation
988 gradient in Peruvian forests, *New Phytol.*, 189, 967-977, [http://dx.doi.org/10.1111/j.1469-
989 8137.2010.03521.x](http://dx.doi.org/10.1111/j.1469-8137.2010.03521.x), 2011.
- 990 Scheel, M. L. M., Rohrer, M., Huggel, C., Santos Villar, D., Silvestre, E., and Huffman, G. J.: Evaluation
991 of TRMM Multi-satellite Precipitation Analysis (TMPA) performance in the Central Andes
992 region and its dependency on spatial and temporal resolution, *Hydrol. Earth Syst. Sc.*, 15,
993 2649-2663, <http://dx.doi.org/10.5194/hess-15-2649-2011>, 2011.
- 994 Schellekens, J.: CQ-FLOW: A distributed hydrological model for the prediction of impacts of land-
995 cover change, with spatial reference to the Rio Chiquito catchment, northwest Costa Rica,
996 CQ-FLOW: A distributed hydrological model for the prediction of impacts of land-cover
997 change, with spatial reference to the Rio Chiquito catchment, northwest Costa Rica, Vrije
998 Universiteit Amsterdam and Forestry Research Programme, Amsterdam, The Netherlands,
999 71 pp., 2006.
- 1000 Schmid, S., Burkard, R., Frumau, K. F. A., Tobon, C., Buijnzeel, L. A., Siegwolf, R., and Eugster, W.:
1001 The wet-canopy water balance of a Costa Rican cloud forest during the dry season, in:
1002 *Tropical Montane Cloud Forests: Science for Conservation and Management*, edited by:
1003 Buijnzeel, L. A., Scatena, F. N., and Hamilton, L. S., Cambridge University Press, Cambridge,
1004 UK, 302-308, 2010.
- 1005 Scholl, M., Eugster, W., and Burkard, R.: Understanding the role of fog in forest hydrology: stable
1006 isotopes as tools for determining input and partitioning of cloud water in montane forests,
1007 *Hydrol. Process.*, 25, 353-366, <http://dx.doi.org/10.1002/hyp.7762>, 2011.
- 1008 Scholl, M. A., Giambelluca, T. W., Gingerich, S. B., Nullet, M. A., and Loope, L. L.: Cloud water in
1009 windward and leeward mountain forests: The stable isotope signature of orographic cloud
1010 water, *Water Resour. Res.*, 43, W12411, <http://dx.doi.org/10.1029/2007WR006011>, 2007.
- 1011 Scholl, M. A., and Murphy, S. F.: Precipitation isotopes link regional climate patterns to water supply
1012 in a tropical mountain forest, eastern Puerto Rico, *Water Resour. Res.*, 50, 4305-4322,
1013 <http://dx.doi.org/10.1002/2013WR014413>, 2014.
- 1014 SENAMHI: Clima: Datos históricos Peru, http://www.senamhi.gob.pe/main_mapa.php?t=dHi, (last
1015 access: May 2012), 2012.
- 1016 Squeo, F. A., Warner, B. G., Aravena, R., and Espinoza, D.: Bofedales: high altitude peatlands of the
1017 central Andes, *Rev. Chil. Hist. Nat.*, 79, 245-255, 2006.
- 1018 Stallard, R. F., and Edmond, J. M.: Geochemistry of the Amazon: 2. The influence of geology and
1019 weathering environment on the dissolved load, *J. Geophys. Res.-Oceans*, 88, 9671-9688,
1020 <http://dx.doi.org/10.1029/JC088iC14p09671>, 1983.
- 1021 Teh, Y. A., Diem, T., Jones, S., Huaraca Quispe, L. P., Baggs, E., Morley, N., Richards, M., Smith, P., and
1022 Meir, P.: Methane and nitrous oxide fluxes across an elevation gradient in the tropical
1023 Peruvian Andes, *Biogeosciences*, 11, 2325-2339, [http://dx.doi.org/10.5194/bg-11-2325-
1024 2014](http://dx.doi.org/10.5194/bg-11-2325-2014), 2014.
- 1025 Thome, C. R., and Zevenbergen, L. W.: Estimating mean velocity in mountain rivers, *J. Hydraul. Eng.*,
1026 111, 612-624, 1985.

- 1027 Thorburn, P. J., Hatton, T. J., and Walker, G. R.: Combining measurements of transpiration and stable
 1028 isotopes of water to determine groundwater discharge from forests, *J Hydrol.*, 150, 563-587,
 1029 [http://dx.doi.org/10.1016/0022-1694\(93\)90126-T](http://dx.doi.org/10.1016/0022-1694(93)90126-T), 1993.
- 1030 Timbe, E., Windhorst, D., Crespo, P., Frede, H. G., Feyen, J., and Breuer, L.: Understanding
 1031 uncertainties when inferring mean transit times of water through tracer-based lumped-
 1032 parameter models in Andean tropical montane cloud forest catchments, *Hydrol. Earth Syst.*
 1033 *Sc.*, 18, 1503-1523, <http://dx.doi.org/10.5194/hess-18-1503-2014>, 2014.
- 1034 Tipper, E. T., Bickle, M. J., Galy, A., West, A. J., Pomiès, C., and Chapman, H. J.: The short term
 1035 climatic sensitivity of carbonate and silicate weathering fluxes: insight from seasonal
 1036 variations in river chemistry, *Geochim. Cosmochim. Ac.*, 70, 2737-2754,
 1037 <http://dx.doi.org/10.1016/j.gca.2006.03.005>, 2006.
- 1038 Todd, D. K., and Mays, L. W.: *Groundwater Hydrology*, 3, Wiley, New York, 625 pp., 1980.
- 1039 Tognetti, S., Aylward, B., and Bruijnzeel, L. A.: Assessment needs to support the development of
 1040 arrangements for payments for ecosystem services from tropical montane cloud forests, in:
 1041 *Tropical Montane Cloud Forests. Science for Conservation and Management*, edited by:
 1042 Bruijnzeel, L. A., Scatena, F. N., and Hamilton, L. S., Cambridge University Press, Cambridge,
 1043 UK, 671-685, 2010.
- 1044 Torres, M. A., West, A. J., and Clark, K. E.: Geomorphic regime modulates hydrologic control of
 1045 chemical weathering in the Andes-Amazon, *Geochim Cosmochim Ac.*, in review.
- 1046 Tovar, C., Arnillas, C. A., Cuesta, F., and Buytaert, W.: Diverging responses of tropical Andean biomes
 1047 under future climate conditions, *PloS one*, 8, e63634,
 1048 <http://dx.doi.org/10.1371/journal.pone.0063634>, 2013.
- 1049 Townsend-Small, A., McClain, M. E., Hall, B., Noguera, J. L., Llerena, C. A., and Brandes, J. A.:
 1050 Suspended sediments and organic matter in mountain headwaters of the Amazon River:
 1051 Results from a 1-year time series study in the central Peruvian Andes, *Geochim. Cosmochim.*
 1052 *Ac.*, 72, 732-740, <http://dx.doi.org/10.1016/j.gca.2007.11.020>, 2008.
- 1053 TRMM: Tropical Rainfall Measuring Mission product 3B43 v7a, NASA,
 1054 [http://mirador.gsfc.nasa.gov/cgi-](http://mirador.gsfc.nasa.gov/cgi-bin/mirador/presentNavigation.pl?tree=project&project=TRMM&dataGroup=Gridded&data)
 1055 [bin/mirador/presentNavigation.pl?tree=project&project=TRMM&dataGroup=Gridded&data](http://mirador/presentNavigation.pl?tree=project&project=TRMM&dataGroup=Gridded&data)
 1056 [set=3B43:%20Monthly%200.25%20x%200.25%20degree%20merged%20TRMM%20and%20](http://mirador/presentNavigation.pl?tree=project&project=TRMM&dataGroup=Gridded&data)
 1057 [other%20sources%20estimates&version=006](http://mirador/presentNavigation.pl?tree=project&project=TRMM&dataGroup=Gridded&data), access: 2 April 2013, 2013.
- 1058 van de Weg, M. J., Meir, P., Grace, J., and Ramos, G. D.: Photosynthetic parameters, dark respiration
 1059 and leaf traits in the canopy of a Peruvian tropical montane cloud forest, *Oecologia*, 168, 23-
 1060 34, <http://dx.doi.org/10.1007/s00442-011-2068-z>, 2012.
- 1061 van de Weg, M. J., Meir, P., Williams, M., Girardin, C., Malhi, Y., Silva-Espejo, J., and Grace, J.: Gross
 1062 primary productivity of a high elevation tropical montane cloud forest, *Ecosystems*, 17, 751-
 1063 764, <http://dx.doi.org/10.1007/s10021-014-9758-4>, 2014.
- 1064 Wilcox, B. P., Allen, B., and Bryant, F.: Description and classification of soils of the high-elevation
 1065 grasslands of central Peru, *Geoderma*, 42, 79-94, 1988.
- 1066 Windhorst, D., Waltz, T., Timbe, E., Frede, H. G., and Breuer, L.: Impact of elevation and weather
 1067 patterns on the isotopic composition of precipitation in a tropical montane rainforest,
 1068 *Hydrol. Earth Syst. Sci.*, 17, 409-419, <http://dx.doi.org/10.5194/hess-17-409-2013>, 2013.
- 1069 Wittmann, H., von Blanckenburg, F., Maurice, L., Guyot, J.-L., Filizola, N., and Kubik, P. W.: Sediment
 1070 production and delivery in the Amazon River basin quantified by in situ-produced
 1071 cosmogenic nuclides and recent river loads, *Geol. Soc. Am. Bull.*, 123, 934-950,
 1072 <http://dx.doi.org/10.1130/b30317.1>, 2011.
- 1073 Zadroga, F.: The hydrological importance of a montane cloud forest area of Costa Rica, in: *Tropical*
 1074 *agricultural hydrology*, edited by: Lal, R., and Russell, E. W., Wiley and Sons, New York, 59-
 1075 73, 1981.
- 1076 Zimmermann, M., Meir, P., Bird, M. I., Malhi, Y., and Ccahuana, A. J. Q.: Climate dependence of
 1077 heterotrophic soil respiration from a soil-translocation experiment along a 3000 m tropical

1078 forest altitudinal gradient, Eur. J. Soil Sci., 60, 895-906, [http://dx.doi.org/10.1111/j.1365-](http://dx.doi.org/10.1111/j.1365-2389.2009.01175.x)
1079 [2389.2009.01175.x](http://dx.doi.org/10.1111/j.1365-2389.2009.01175.x), 2009.

1080

1081

1082

1083

1084

1085 **Tables**

1086

TABLE 1: Descriptions of the Kosñipata catchment.

Catchment	Area (km ²)	Mean slope* (°)	Mean elevation* (masl)	Elevation range* (masl)	Landcover type [‡] (~ %)	Geology [^] (~ %)	Gauge lat/long (S, W)	Gauge elevation (masl)
Kosñipata at San Pedro	164.4	28	2805	1360 to 4000	TMCF (<u>92.7</u>), puna /transition (<u>7.3</u>)	mudstones (80), pluton intrusions (20)	13°3'37", 71°32'40"	1360
Kosñipata at Wayqecha**	48.5	26	3195	2250 to 3905	TMCF (<u>75</u>), puna /transition (<u>25</u>)	mudstones (100)	13°9'46", 71°35'21"	2250

* Based on Shuttle Radar Topography Mission (SRTM) data with a 90 m x 90 m resolution.

[^] Basin geology derived from (Carlotto Caillaux et al., 1996).

[‡] Landcover types were determined using 2009 Quickbird 2 imagery.

** Results presented in supplementary information.

1087

1088

TABLE 2: Water budget components for the Kosñipata catchment at the San Pedro (SP) gauging station, for the annual period from February 2010 to January 2011. Percentages indicate fraction of the annual total for that component.

	Number of months/ days	Q (m ³ s ⁻¹)	Runoff mm d ⁻¹ , (%)	Baseflow mm d ⁻¹ (%)	BFI*	Rainfall [^] mm d ⁻¹ (%)	CWI mm d ⁻¹ (%)	AET mm d ⁻¹ (%)
Wet	4/ <u>121</u>	23.1±1.3	12.13±0.68 (52)	9.41±0.77 (52)	0.77±0.04	15.00±3.08 (58)	1.37±0.70 (52)	1.87±0.37 (33)
Wet-dry	1/ <u>30</u>	19.6±2.6	10.29±1.37 (11)	8.75±1.35 (12)	0.85±0.02	6.95±2.58 (7)	1.16±1.39 (11)	1.86±0.37 (8)
Dry	5/ <u>153</u>	8.1±0.9	4.31±0.46 (24)	3.58±0.48 (26)	0.83±0.04	4.32±0.73 (21)	0.50±0.32 (24)	1.81±0.36 (40)
Dry-wet	2/ <u>61</u>	11.3±1.5	5.94±0.81 (13)	3.56±0.73 (10)	0.60±0.04	7.02±1.95 (14)	0.63±0.75 (12)	2.11±0.42 (19)
Annual	12/ <u>365</u>	14.6±0.7	7.66±0.35 (100)	5.95±0.37 (100)	0.77±0.04	8.53±1.13 (100)	0.87±0.32 (100)	1.88±0.38 (100)

Seasonal contribution as percentage of total in parenthesis.

Uncertainties are propagated 1σ errors.

* Base flow index (BFI) is the ratio of the total volume of baseflow divided by the total volume of discharge following the method outlined in Gustard et al. (1992).

[^] Catchment-wide rainfall is corrected for wind-induced loss and is reported for February 2010 to January 2011 to coincide with the study period.

1089

1090

TABLE 3: Breakdown of streamflow into its sources

	n	Fraction wet season rainfall ^a	Fraction dry season rainfall ^a	Fraction cloud water ^a	Wet season rain as a source (mm month ⁻¹) ^b	Dry season rain as a source (mm month ⁻¹) ^b	Cloud water as a source (mm month ⁻¹) ^b	Total stream runoff (mm month ⁻¹)
Feb-10	28	0.62±0.04	0.24±0.04	0.11±0.03	231±16	91±17	41±13	372±38
Mar-10	2	0.62±0.15	0.25±0.16	0.10±0.12	261±70	105±72	44±56	420±41
Apr-10	2	0.65±0.14	0.21±0.14	0.11±0.12	200±49	66±49	35±42	309±41
May-10	3	0.61±0.12	0.25±0.13	0.11±0.10	143±34	59±35	27±28	235±40
Jun-10	1	0.63±0.20	0.22±0.20	0.12±0.17	103±40	36±40	19±35	163±35
Jul-10	2	0.58±0.13	0.28±0.14	0.12±0.11	61±17	28±18	13±14	105±30
Aug-10	3	0.58±0.13	0.27±0.14	0.12±0.10	51±15	24±16	10±12	87±26
Sep-10	3	0.59±0.13	0.26±0.23	0.12±0.11	42±12	19±13	8±10	70±23
Oct-10	1	0.64±0.22	0.26±0.23	0.08±0.16	127±53	51±55	16±39	199±36
Nov-10	3	0.52±0.14	0.30±0.15	0.14±0.12	86±28	50±31	23±25	164±34
Dec-10	4	0.56±0.12	0.30±0.13	0.10±0.09	188±44	98±50	35±33	333±42
Jan-11	2	0.55±0.16	0.29±0.18	0.14±0.14	186±62	99±69	46±54	339±43
Fractional contributions by season ^c								
Wet		0.59±0.07	0.27±0.08	0.11±0.05				
Wet-dry		0.65±0.14	0.21±0.14	0.11±0.12				
Dry		0.61±0.09	0.25±0.09	0.12±0.07				
Dry-wet		0.59±0.16	0.28±0.17	0.11±0.13				
Annual		0.60±0.05	0.26±0.05	0.11±0.04				

^a Calculated from monthly average values of mixing model results. Reported errors are propagated uncertainty (1σ) from individual samples per month, accounting for uncertainties from the Monte Carlo mixing model (Table S7 in the Supplement).

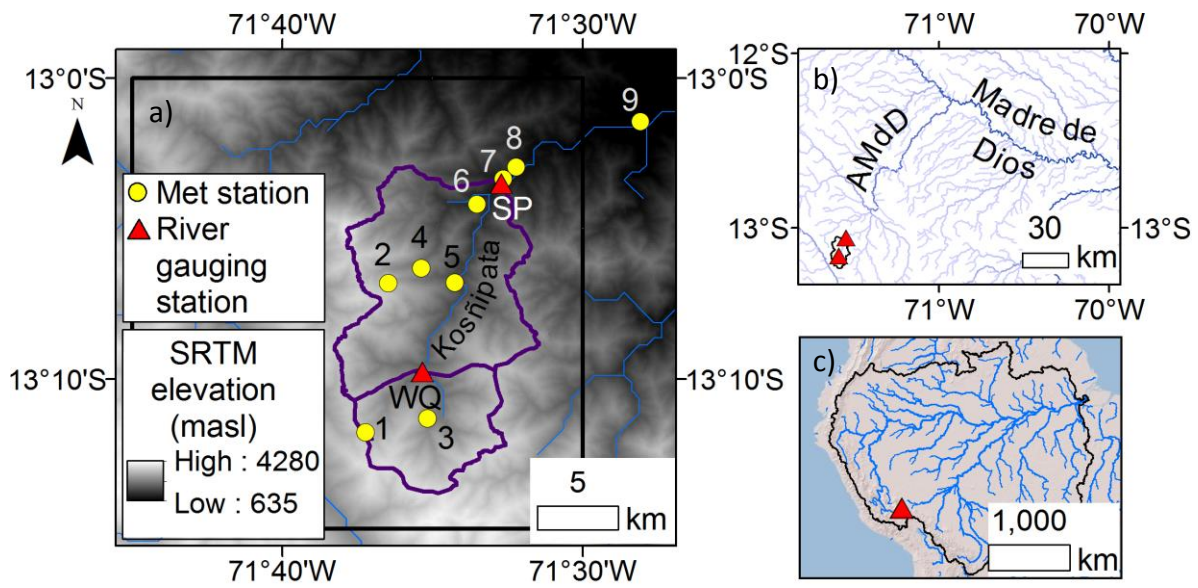
^b Calculated from monthly fractional contributions and monthly runoff. Reported errors are propagated uncertainty (1σ) from the mixing modelling and from the variation in stream runoff.

^c Calculated based on runoff totals for each month, from each source, summed for a given season. Reported errors are propagated uncertainty from monthly runoff estimates from each source.
 n = number of samples.

1091

1092

1093 **Figures**



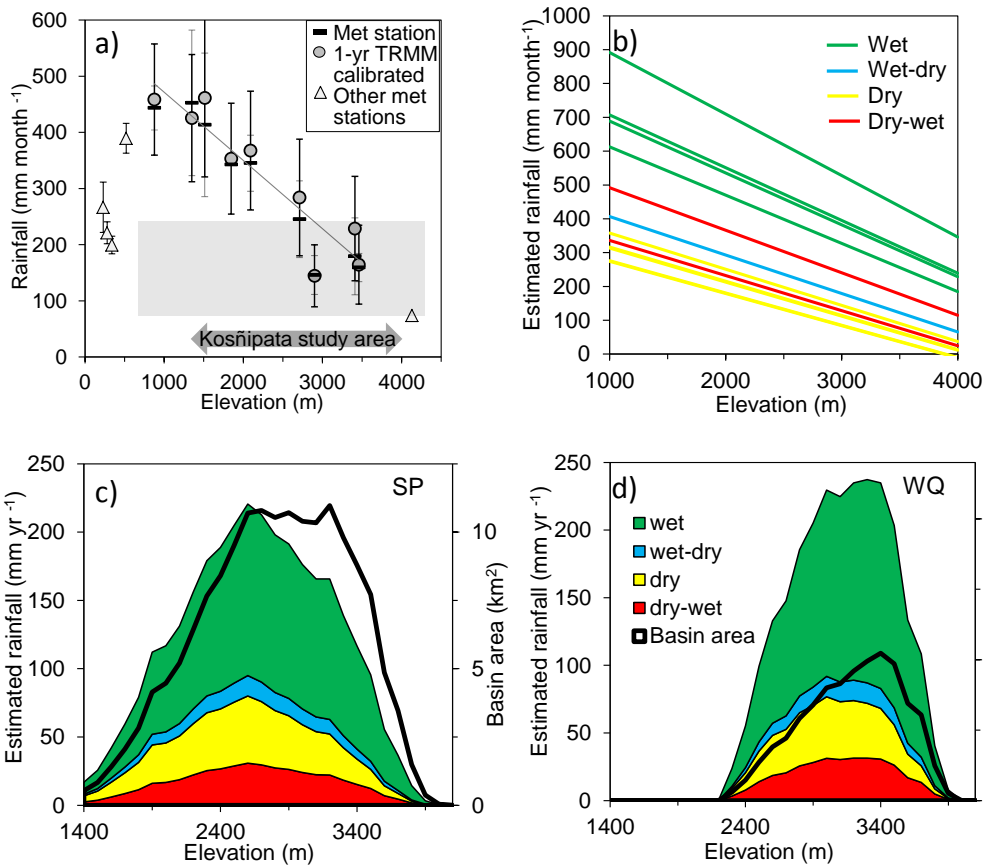
1094

1095 | Figure 1: a) The Kosñipata catchment, Eastern Andes of Peru, showing the Kosñipata River
1096 catchment measured at the San Pedro (SP) river gauging station and the nested sub-catchment
1097 at the Wayqecha (WQ) river gauging station, overlaid on 90 m x 90 m digital elevation
1098 model (Shuttle Radar Topography Mission) (Farr et al., 2007). Black box indicates the extent
1099 of the TRMM 3B43 tile used in this study (cf. Fig. 2a). The meteorological stations used for
1100 rainfall data are numbered 1 to 9 (Table S2). b) The Kosñipata River flows into the Alto
1101 Madre de Dios (AMdD) and then into the Madre de Dios River, a major tributary of the
1102 Amazon River (c). The river network was produced from HydroSHEDS (hydrological data
1103 and maps based on shuttle elevation derivatives at multiple scales) (Lehner et al., 2008).

1104

1105

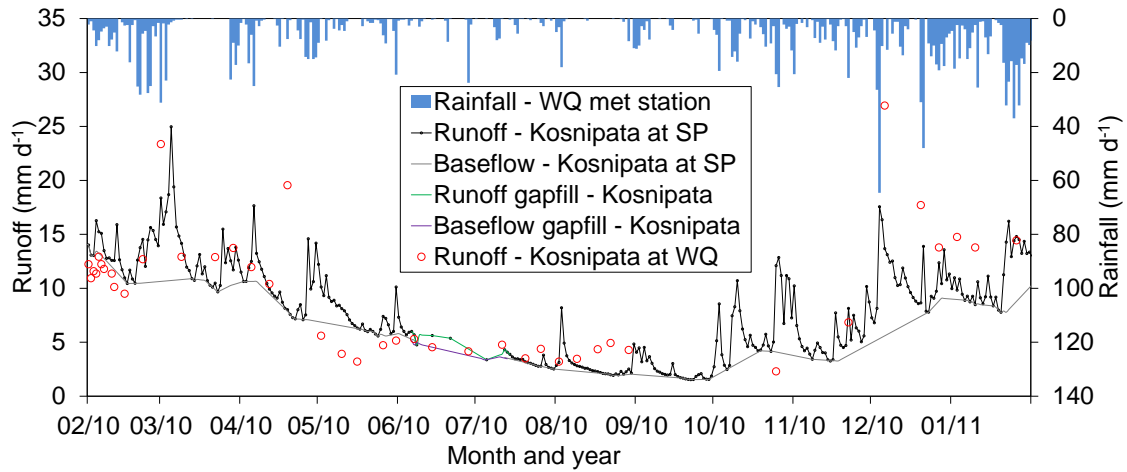
1106



1107

1108

1109 Figure 2: Mean monthly rainfall data for the 9 meteorological stations in the Kosñipata
 1110 catchment study area (from ~900 to ~3500 masl) (dark dashes and light error bars) and
 1111 estimated mean monthly rainfall (grey circles and dark error bars) covering the months of the
 1112 1-year study period (February 2010 to January 2011) determined using the linear regression
 1113 equations for each meteorological station derived from tropical rainfall measuring mission
 1114 (TRMM) data (Table S8). The grey line is the linear fit with elevation for the estimated mean
 1115 monthly rainfall ($\text{mm month}^{-1} = -0.1216 \pm 0.0187 \times \text{elevation} + 593.16 \pm 44.94$, $R^2 = 0.86$; $P =$
 1116 0.0003). The error bars are $2 \times$ standard error of monthly data. Mean monthly rainfall for 5
 1117 meteorological stations outside of the study area but within the larger Madre de Dios Basin
 1118 are also shown as triangles (Rapp and Silman, 2012). The shaded box shows the TRMM
 1119 3B43 v7a monthly mean rainfall for the 1-year study period with $2 \times$ standard error.
 1120 Elevation range is shown for the $34.5 \text{ km} \times 34.5 \text{ km}$ TRMM tile. The altitudinal range of the
 1121 study area is represented by the dashed lines at 1350 and 4000 masl. b) Linear regressions of
 1122 estimated catchment wide rainfall by month from February 2010 to January 2011, colour-
 1123 coded by season. The distribution of annual rainfall with elevation by season for the
 1124 Kosñipata River is shown for the San Pedro (SP) gauging station (c) and the Wayqecha (WQ)
 1125 gauging station (d) at 100 m intervals using the monthly linear regressions (b) incorporating
 1126 the correction for wind-induced rainfall loss (Table S3).

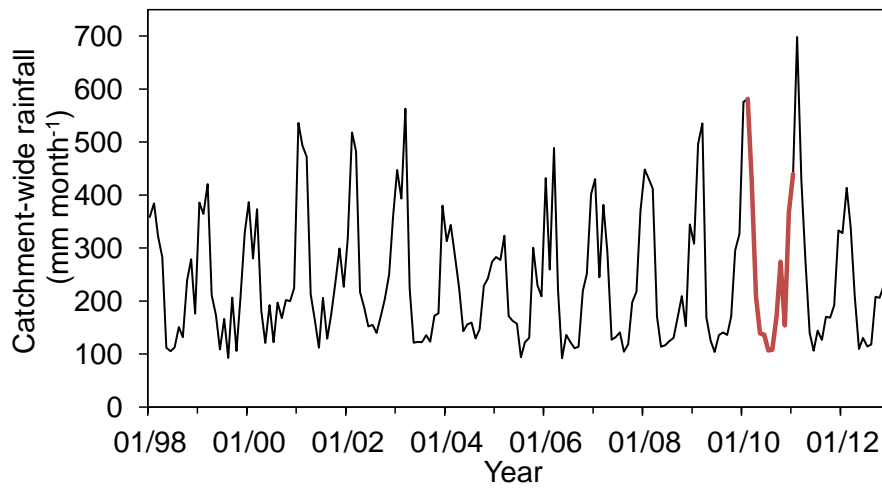


1127

1128 Figure 3: Runoff for the Kosñipata River at the San Pedro (SP) and Wayqecha (WQ) gauging
 1129 stations. Rainfall (top axis) from the Wayqecha meteorological station is on the secondary
 1130 axis. The Kosñipata River runoff at San Pedro and baseflow were measured nearly
 1131 continuously through the year, with a 31-day gap partly in July and August that is covered by
 1132 three manual measurements and the gap filled using linear interpolation. The Kosñipata River
 1133 runoff at Wayqecha was measured throughout the year from a daily to a monthly interval and
 1134 is discussed in the supplementary section.

1135

1136



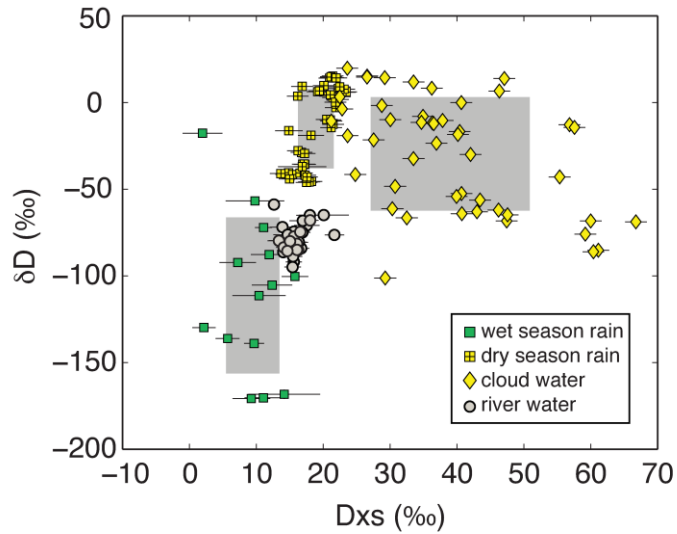
1137

1138

1139 Figure 4: Catchment wide TRMM calibrated rainfall for the Kosñipata catchment from 1998
1140 to 2012. The thick red line represents the 1-year study period.

1141

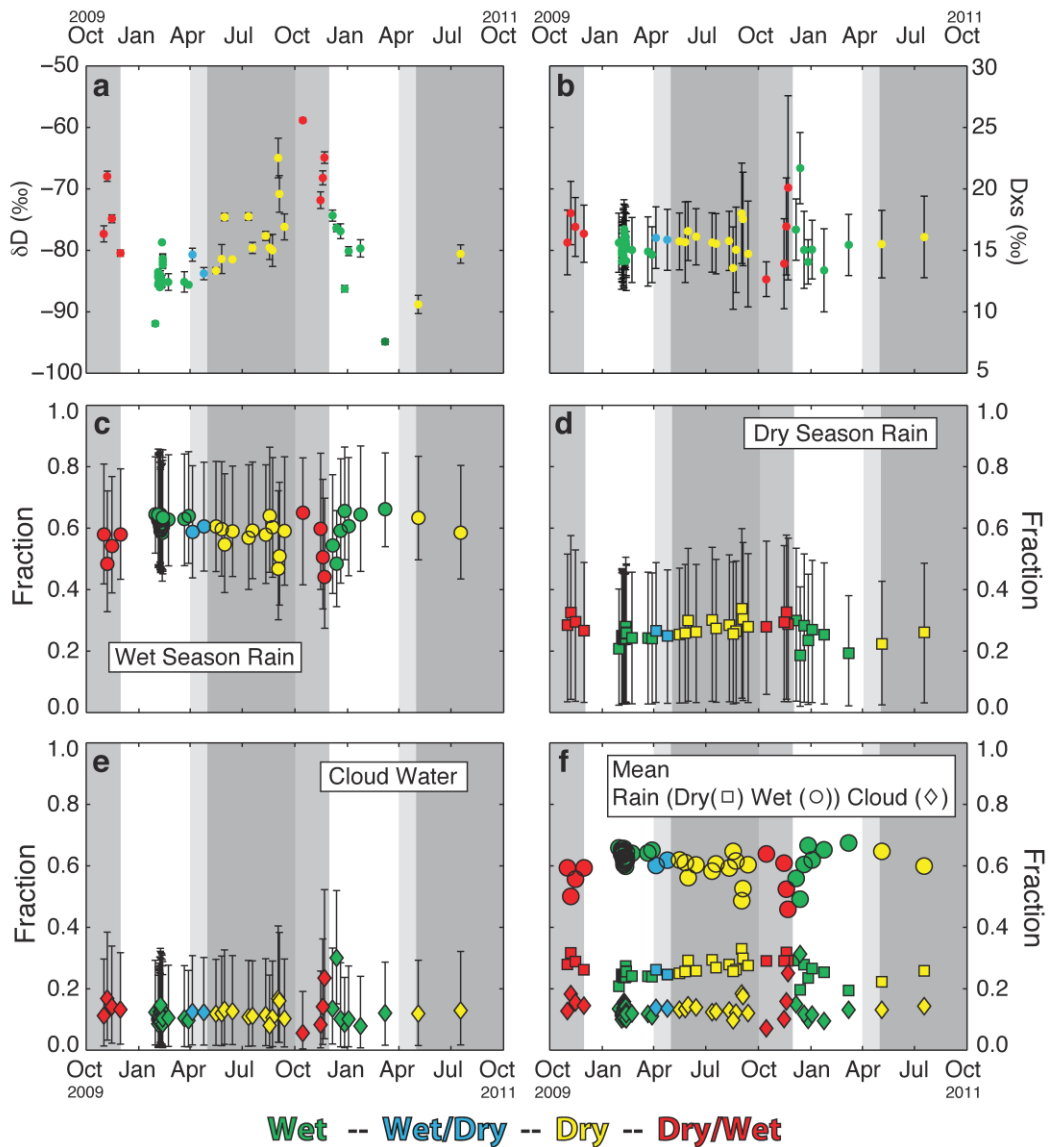
1142



1143

1144 Figure 5: Hydrogen isotope ratio (δD , ‰) and deuterium excess (Dxs , ‰) of dry season
1145 cloud water vapour (yellow diamonds), and river water (grey circles) from the Kosñipata
1146 catchment. Rainwater samples (squares) are from the dry season (May to August, yellow) and
1147 from the wet season (December to March, green). All error bars correspond to two standard
1148 deviations. The grey shaded regions encompass the mean δD and Dxs values and one
1149 standard deviation for each end-member (i.e. wet season rainfall, dry season rainfall, and dry
1150 season cloud water vapour). The ranges defined by these grey boxes were used to generate
1151 random sets of end-member compositions for the three end-member mixing model.

1152



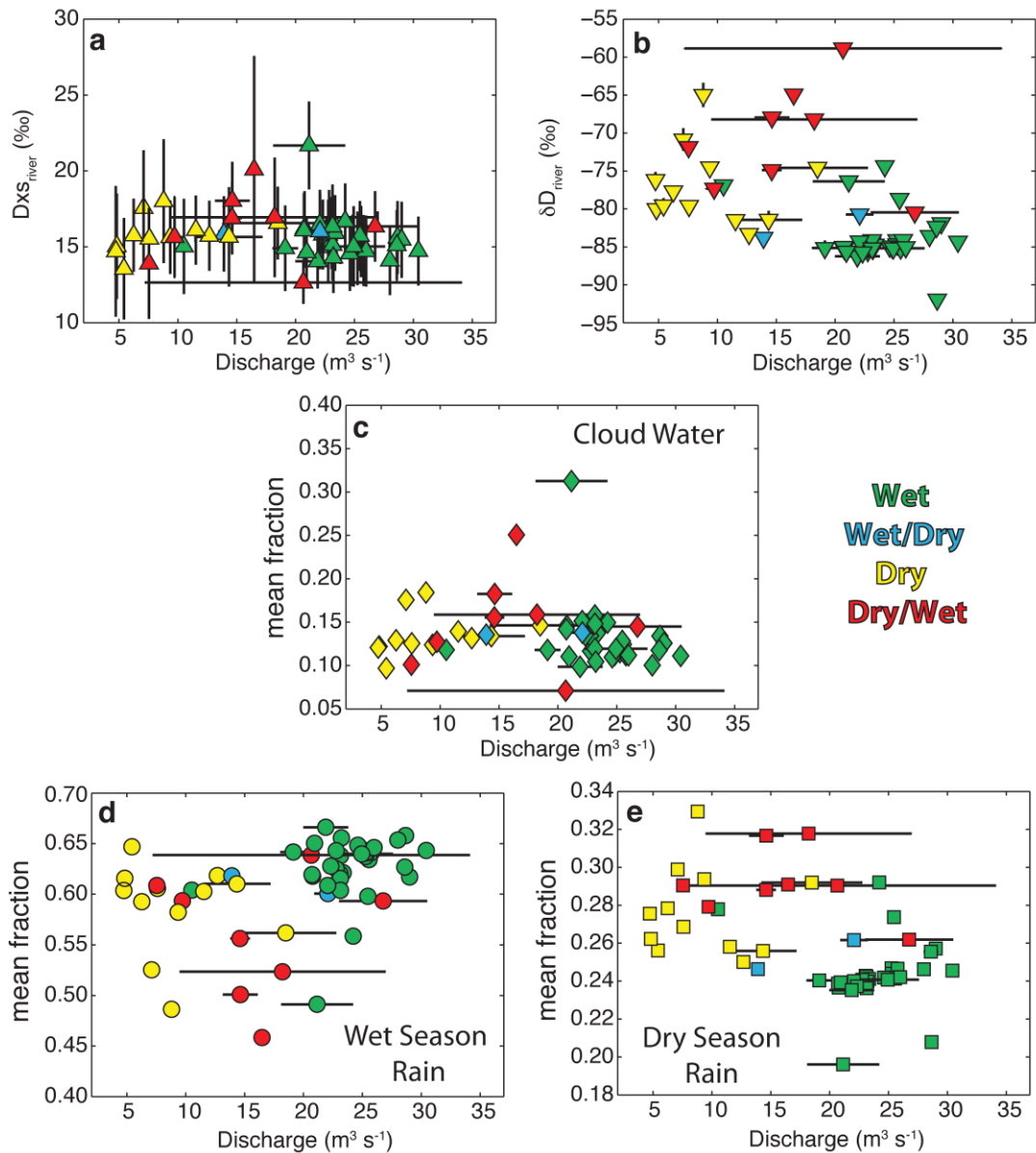
1153

1154 Figure 6: Time series of river water hydrogen isotopes (δD_{river}) and river water deuterium
 1155 excess (Dx_{Sriver}), and the calculated mixing proportions of different sources for the Kosñipata
 1156 River. a) The time series of δD_{river} values with error bars signifying 2 standard deviations. b)
 1157 The time series of Dx_{Sriver} values with error bars signifying 2 standard deviations. Time series
 1158 of the 5th (lower error bar), 50th (open circle), and 95th percentile (upper error bar) values of
 1159 the distribution of fractional contributions to river discharge, calculated using the three end
 1160 member mixing model, of: c) wet season rain; d) dry season rain; and e) cloud water vapour.
 1161 f) Time series of the mean contributions of wet season rain (circle), dry season rain (square),
 1162 and cloud water vapour (diamond) to river discharge.

1163

1164

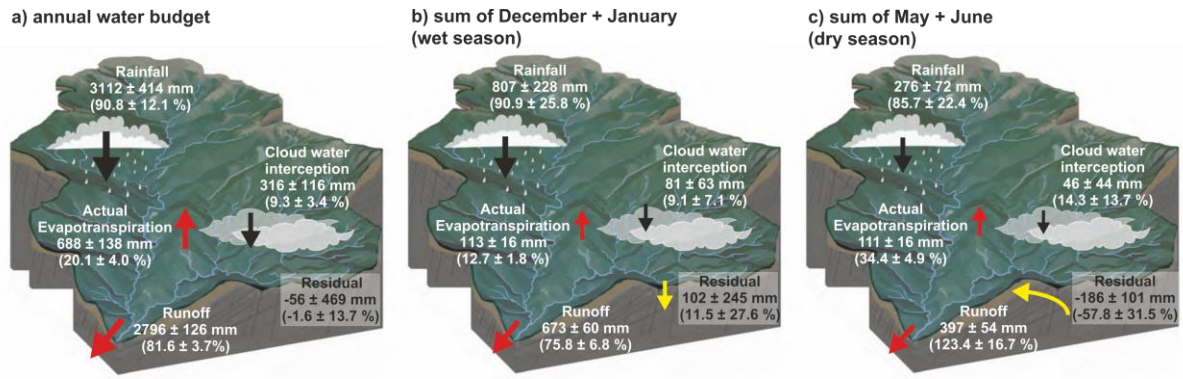
1165



1166

1167 Figure 7: Variation in the isotopic composition of river water a) deuterium excess ($Dx_{s_{river}}$,
 1168 ‰) and b) hydrogen isotope ratio (δD_{river} , ‰) plotted versus discharge ($m^3 s^{-1}$). Variation in
 1169 the mean contributions to river flow as a function of water discharge for cloud water vapour
 1170 (c), wet season rain (d), and dry season rain (e) as calculated by the end member mixing
 1171 analysis, also plotted versus discharge.

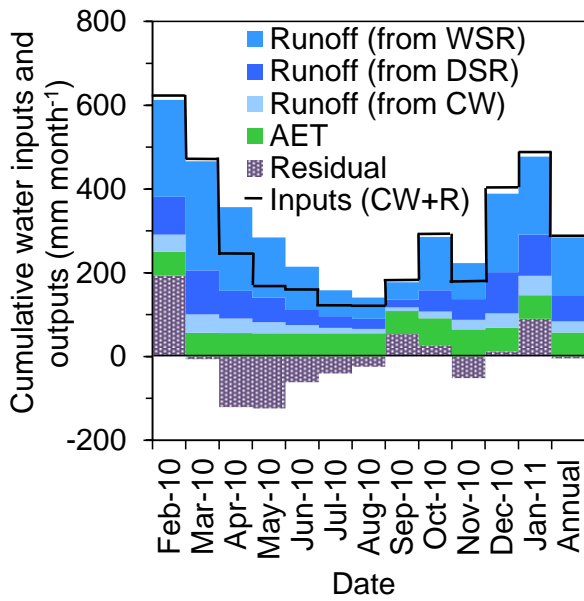
1172



1173
1174
1175
1176
1177
1178
1179
1180
1181
1182
1183

Figure 8: A schematic illustration of the water budget for the Kosñipata catchment for (a) the study year, (b) the early wet season (December and January), and (c) the early dry season (May and June). Black arrows represent inputs and red arrows represent outputs; yellow arrows represent the reversible flux of the residual over the wet and dry seasons, reflecting the transient seasonal storage of water in soil and fractured bedrock (see Discussion in text). The sizes of the arrows are scaled logarithmically with the magnitude of the flux. Values indicated are sums for that time period in mm.

1184



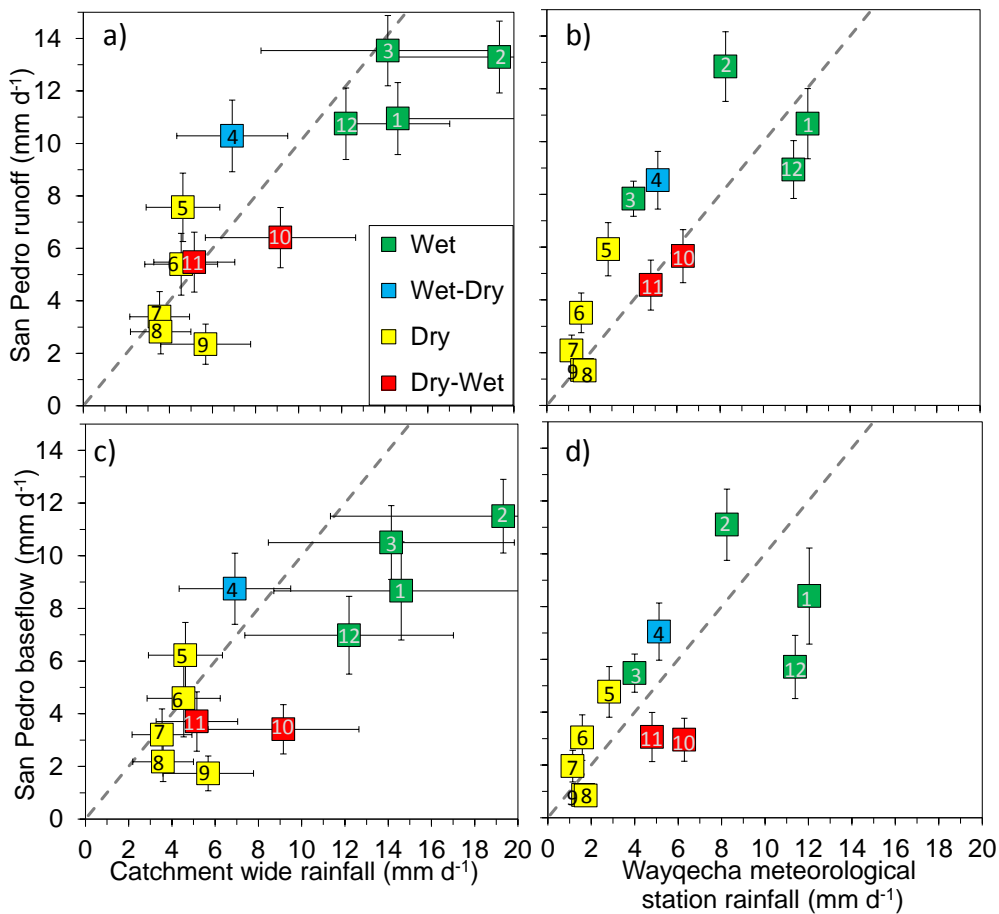
1185

1186 | Figure 9: Cumulative water inputs (rainfall and cloud water interception) are represented by
1187 the black line. Cumulative water outputs (river runoff and actual evapotranspiration) and the
1188 residual are separated out into cumulative coloured stacked bars. Runoff is separated into its
1189 3 sources: wet season rainfall (WSR), dry season rainfall (DSR), and cloudwater (CW)
1190 (Table 3). The study period is separated by month and the monthly balance is determined for
1191 the study year, February 2010 to January 2011.

1192

1193

1194



1195

1196

1197 Figure 10: Mean monthly rainfall (corrected for wind-induced loss) versus river runoff (mm
1198 d⁻¹) for the Kosñipata catchment, showing anticlockwise hysteresis throughout the year, with
1199 months numbered chronologically and colour coded by season (see Figs. 2 & 7). Plots show
1200 stream runoff versus a) catchment wide rainfall and b) meteorological station rainfall for the
1201 Wayqecha meteorological station (2900 masl), and baseflow versus c) catchment wide
1202 rainfall and d) meteorological station rainfall at Wayqecha. Error bars represent one standard
1203 deviation. The one-to-one line for rainfall to river runoff is represented by the grey dashed
1204 line. Note: in b) and d) days with zero rainfall were excluded as per the approach used by
1205 Andermann et al. (2012).